Journal of Environmental Management 236 (2019) 695–714

Contents lists available at ScienceDirect

Journal of Environmental Management

journal homepage: www.elsevier.com/locate/jenvman

Research article

Hydrodynamic modelling of a polluted tropical bay: Assessment of anthropogenic impacts on freshwater runoff and estuarine water renewal

Marko Tosic[a,b,d,*], Flávio Martins[b], Serguei Lonin[c], Alfredo Izquierdo[a], Juan Darío Restrepo[d]

[a] University of Cádiz, Faculty of Marine and Environmental Sciences, Applied Physics Department, 11510, Puerto Real, Cádiz, Spain
[b] Instituto Superior de Engenharia, Universidade do Algarve, Campus da Penha, 8000, Faro, Portugal
[c] Escuela Naval de Cadetes "Almirante Padilla", Isla Naval Manzanillo, Cartagena de Indias, Colombia
[d] Universidad EAFIT, School of Sciences, Department of Earth Sciences, Carrera 49 #7S-50, A.A.3300, Medellín, Colombia

ARTICLE INFO

Keywords:
3D hydrodynamic modelling
Water renewal time scales
Vertical mixing
Estuarine circulation
Semi-enclosed coastal waters
Environmental management

ABSTRACT

A bay's capacity to buffer fluvial fluxes between the land and sea is sensitive to hydrological changes that can affect its water renewal rates. In Cartagena Bay, Colombia, pollution issues have been associated with freshwater fluxes which are projected to increase in future years. This has led to plans to reduce freshwater flows by constructing upstream hydraulic doors. Given the influence of freshwater discharge on coastal water renewal, it is important to assess how these upstream changes will affect the bay's hydrodynamic processes. This study calibrated the 3D MOHID Water model, configured with a high-resolution mixed vertical discretization to capture the bay's characteristic processes of vertical stratification and mixing. A Lagrangian transport model was used to analyze the flow of passive particle tracers and calculate water renewal time scales. Mean residence times of 3–6 days and flushing times of 10–20 days for canal water were found, while mean residence times of 23–33 days and flushing times of 70–99 days were calculated for the bay's complete water volume. An assessment of future scenarios showed that increases in freshwater runoff would result in faster water renewal in the bay, while plans to decrease freshwater discharge would result in slower water renewal in the bay. It is therefore imperative that any plans for reducing fluvial fluxes into the bay be accompanied by the control of local pollution sources, which are abundant and could worsen the bay's water quality issues should water renewal times become longer.

1. Introduction

Balance is a concept on which various scientific and philosophic theories are based. Physicists rely on the principle of mass conservation to balance the fluxes of pollution models, economic theories are contingent on the balance between supply and demand, while Aztec philosophers postulated the importance of living a life in balance with an ephemeral world. Unfortunately for the natural world, the concept of balance is seldom prominent in the reality of human resource use, as currently there is no country that meets the basic needs of its citizens within globally sustainable levels (O'Neill et al., 2018). Among the natural resources that are particularly vulnerable are coastal semi-enclosed water bodies, which possess valuable ecosystem services that provide for human livelihoods and wellbeing (Newton et al., 2014, 2018). One such water body is Cartagena Bay (Fig. 1), Colombia, where human development has led to the eradication of coral reefs and seagrass communities (Díaz and Gómez, 2003; Restrepo et al., 2006; Restrepo, 2008) and continues to cause multifactorial pollution impacts, including hypoxic conditions and drastic reductions in artisanal fisheries (Tosic et al., 2019, 2018).

Cartagena (Fig. 1) is indeed a "hot-spot" in terms of pollution, tourism and human development. This coastal city is home to a population of one million people, has one of the country's largest ports and industrial zones, and represents Colombia's principal touristic destination. Various problems related to the waters, sediments and biota of Cartagena Bay have been observed for decades, including excessive turbidity, eutrophication, hypoxia, fecal contamination, presence of heavy metals, hydrocarbons and pesticides (FAO & CCO, 1978; Garay, 1983: Guerrero et al., 1995; Castro, 1997; Garay and Giraldo, 1997; Alonso et al., 2000; Parga-Lozano et al., 2002; Tuchkovenko and Lonin, 2003; Restrepo et al., 2006, 2016; Cañon Páez et al., 2007; Johnson-Restrepo et al., 2008; Olivero-Verbel et al., 2008, 2009; 2013; Cogua et al., 2012; Mogollón, 2013; Jaramillo-Colorado et al., 2015, 2016; Tosic et al., 2019). While the bay's water quality issues have been linked to local domestic and industrial wastewater, as well as continental sources of pollution (Tosic et al., 2018), foremost to these

* Corresponding author. University of Cádiz, Faculty of Marine and Environmental Sciences, Applied Physics Department, 11510, Puerto Real, Cádiz, Spain.
E-mail addresses: marko.tosic7@gmail.com, mtosic@eafit.edu.co (M. Tosic).

https://doi.org/10.1016/j.jenvman.2019.01.104
Received 28 August 2018; Received in revised form 8 December 2018; Accepted 26 January 2019
Available online 14 February 2019
0301-4797/

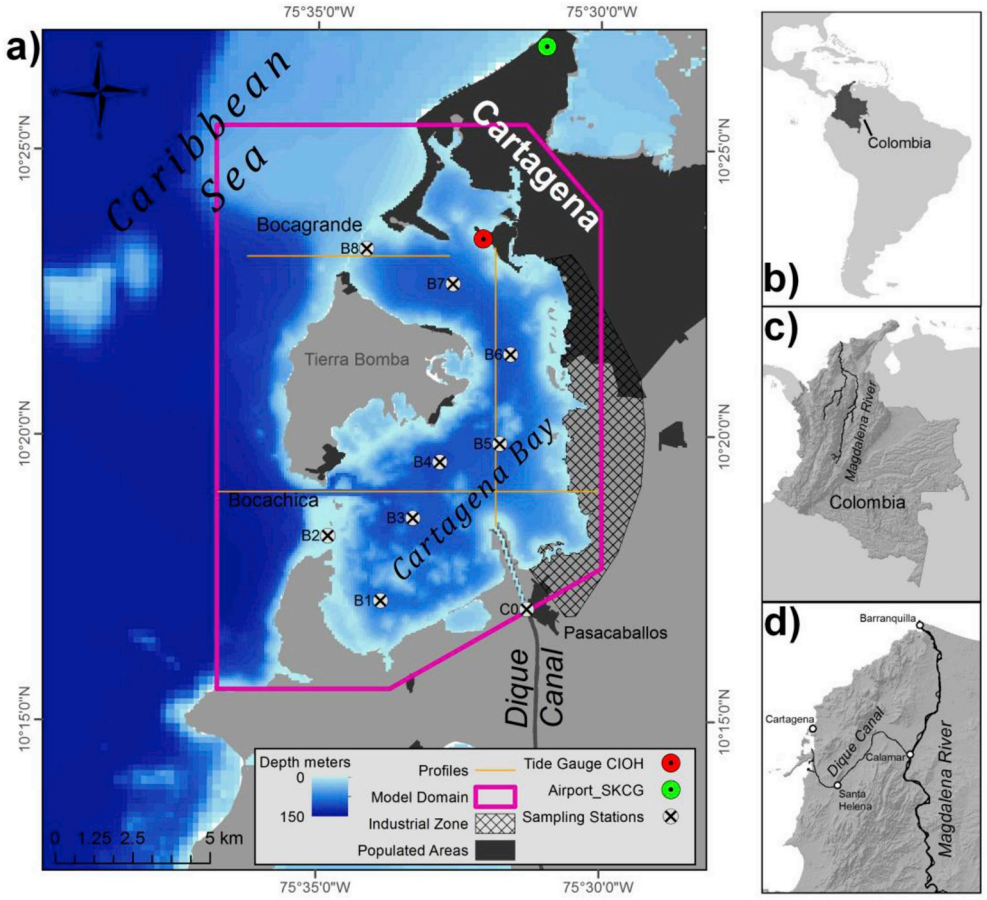

Fig. 1. a) Study area showing sampling stations (C0, B1-8), weather station (SKCG), tide station, bathymetry, model domain and profiles extracted from model results (Figs. 5 and 6). b) Location of Colombia. c) Location of the Magdalena River. d) Flow of the Magdalena into the Caribbean Sea and along the Dique Canal into Cartagena Bay.

sources is runoff from the Dique Canal flowing from the Magdalena River, which is the principal source of fluvial fluxes discharging in the Caribbean Sea (Restrepo and Kjerfve, 2000; Restrepo, 2008).

Pollution issues have motivated numerous studies of the bay's water circulation and contaminant transport (Pagliardini et al., 1982; Andrade et al., 1988; Urbano et al., 1992). Such observational-based studies when combined synergistically with hydrodynamic and transport models allow a more comprehensive understanding of these phenomena (James, 2002). In Cartagena Bay, the 3-dimensional hydrodynamic model CODEGO was developed and used to study various processes: hydrodynamics and sediment transport (Lonin, 1997a; Lonin and Tuchkovenko, 1998; Lonin et al., 2004); eutrophication and oxygen regimes (Lonin and Tuchkovenko, 1998; Tuchkovenko et al., 2000, 2002; Tuchkovenko and Lonin, 2003); oil spills (Lonin, 1997b, 1999; Lonin and Parra, 2005); and pollution due to phenols, fecal coliforms, grease and fats (Lonin, 2009). Other modelling studies in Cartagena Bay have also focused on its water exchange mechanisms (Molares and Mestres, 2012a; Grisales et al., 2014), water levels (Molares and Mestres, 2012b; Andrade et al., 2013, 2017), tidal dynamics (Palacio et al., 2010; Rueda et al., 2013) and sediment distribution (Restrepo et al., 2016).

These modelling studies succeeded in characterizing many of the bay's hydrodynamic and ecological processes. However, no previous study has quantified time scales of water renewal in Cartagena Bay, although some authors have endorsed this need (Gómez et al., 2009; Grisales et al., 2014). Water renewal time scales can effectively reflect a water body's capacity to receive pollution and provide useful information for coastal monitoring and management (Karydis and Kitsiou, 2013). Semi-enclosed coastal water bodies are also particularly vulnerable to changes in water renewal, because these water bodies play the important role of buffering fluxes of water, sediments, nutrients and organisms between the land and sea, and so changes to water renewal rates can alter the ecosystem's composition, sensitivity to eutrophication and ultimately its dissolved oxygen concentrations (Dettmann, 2001; Anthony et al., 2009; Newton et al., 2014).

There are several metrics and terms used for water renewal time scales. Two of the more practical time scales are “residence time” and “flushing time”, however, as differing terminology is occasionally confusing (Jouon et al., 2006), it is important that each study states its chosen definitions. Residence time may be defined as an estimate of the time required for a single water particle to flow out of a water body (Zimmerman, 1976; Takeoka, 1984). Flushing time may be defined as an estimate of the time required to renew a water body's entire volume of water (Steen et al., 2002; Delhez et al., 2004), which has also been termed “turn over time” (Takeoka, 1984). Hydrodynamic models are commonly used to calculate water renewal time scales in semi-enclosed water bodies (Braunschweig et al., 2003; Delhez et al., 2004; Cucco and Umgiesser, 2006; Ferrarin et al., 2013).

Water renewal times are important when considering mitigation strategies that could alter a water body's hydrodynamics (Lee and Park, 2013). In Colombia, there is an ongoing hydraulic intervention that plans to construct hydraulic doors along the Dique Canal and thus reduce flows of freshwater and pollution into Cartagena Bay (Fondo Adaptación, 2018). This intervention has been in discussion for at least 20 years, motivating numerous modelling studies assess the effect that reduced discharge could potentially have on the bay. Analyzing different scenarios of reduced discharge and local pollution control, it was found that reducing the canal's flow into Cartagena Bay would only improve the bay's hypoxic conditions if these actions were also combined with the elimination of local sources of industrial and domestic wastewater (Lonin and Tuchkovenko, 1998; Tuchkovenko et al., 2000, 2002; Tuchkovenko and Lonin, 2003). If these local sources of pollution

were to persist, reductions in freshwater discharge would simply result in greater algal blooms and further oxygen depletion, as the lack of turbid freshwater plumes would increase residence time and improve transparency, allowing primary productivity to flourish with the continued contribution of nutrients from local wastewater (Lonin, 1997a; Tuchkovenko et al., 2000). Yet unfortunately, the city's plan to redirect local wastewater sources out of the bay has fallen behind schedule and significant domestic and industrial pollution loads continue to discharge into the bay (Tosic et al., 2018).

On the other hand, no previous study has modelled scenarios in the bay of increased freshwater discharge from the Dique Canal. Studies of the Magdalena watershed show significant increases in streamflow and sediment load which experienced increases of 24% and 33%, respectively, during the 2000–2010 period compared to the pre-2000 period (Restrepo et al., 2018). Meanwhile, the Canal del Dique witnessed increases in water discharge and sediment load of 28% and 48%, respectively. Based on these trends, hydrological modelling predictions show that water discharge and sediment flux from the Canal del Dique will increase by ~164% and ~260%, respectively, by the year 2020 when compared with the average discharge during the 2000–2010 period. These trends are in close agreement with watershed changes in land-cover and deforestation over the last three decades (Restrepo et al., 2015) and further increases in freshwater discharge could also be expected if future precipitation increases due to climate change and the intensification of the El Niño-Southern Oscillation (IPCC et al., 2014; Paeth et al., 2008; Restrepo et al., 2018).

In this study, we aim to demonstrate the effectiveness of applying a hydrodynamic modelling approach as a tool for the integrated management of coastal waters in a tropical bay. The objective of this approach is to use field monitored data and a calibrated hydrodynamic model to characterize the hydrodynamic processes of water renewal and vertical exchange in Cartagena Bay. The model is then applied to evaluate possible future scenarios in order to answer the following research question: How can upstream anthropogenic impacts on freshwater runoff affect the bay's hydrodynamic processes? By basing its modelling on an extensive monitoring dataset, this study provides local environmental authorities with reliable knowledge on the bay's hydrodynamics and water renewal processes along with a novel tool used to manage these coastal water resources. Further to responding to the management necessities of Cartagena Bay, which holds both socio-economic and ecological relevance to Colombia, the demonstrated approach would be appropriate to apply in similar tropical bays throughout the Caribbean Region where pollution impacts pose an extensive threat to coastal waters, ecosystems, tourism and human health (UNEP/GPA, 2006; UNEP-UCR/CEP, 2010; Jackson et al., 2014).

2. Materials and methods

2.1. Study area

Cartagena Bay is a tropical semi-closed estuary located on the north coast of Colombia, adjacent to the Caribbean Sea (10°20′ N, 75°32′ W, Fig. 1). The bay has a surface area of 84 km^2, including a small internal embayment situated to the north, an average depth of 16 m, a maximum depth of 32 m, a maximum meridian length of 16 km (N-S), and a latitudinal length of 9 km (E-W). The bay is connected to the Caribbean Sea by two straits: “Bocachica” to the south and “Bocagrande” to the north. Movement through the Bocagrande strait is limited by a defensive colonial seawall 2 m below the surface. Bocachica strait consists of a shallow section with depths of 1–3 m as well as a navigation channel which is 100 m wide and 24 m deep (Tuchkovenko and Lonin, 2003; Lonin et al., 2004; Grisales et al., 2014).

Water exchange in the bay is governed by wind-driven circulation and tidal movement through its two seaward straits and the influent discharge of freshwater from the Dique Canal in the south (Molares and Mestres, 2012a). The tides in the bay have a mixed, mainly diurnal signal with a micro-tidal range of 20–50 cm and principal tidal constituents K1 and M2 with amplitudes of 9 and 7 cm, respectively (Molares, 2004). The Dique Canal discharges approximately 55–250 m^3/s of freshwater into the bay (Tuchkovenko and Lonin, 2003), the variability of which is strongly related to the seasonality of runoff from the Magdalena River, from which the Dique Canal diverges at Calamar 114 km upstream of Cartagena Bay. This freshwater discharge produces estuarine conditions in the bay characterized by a highly stratified upper water column with a pronounced pycnocline in the upper 4 m of depth, above which turbid freshwater is restricted from vertical mixing (Tuchkovenko et al., 2000, 2002; Tuchkovenko and Lonin, 2003). Additional sources of freshwater discharging into the bay include wastewater from small populations around the bay and an industrial sector along the bay's east coast (Cardique & AGD, 2006). During local rainy conditions, additional freshwater also enters the bay due to runoff from a small coastal catchment area around the bay, as well as discharge from an outdated submarine outfall (near station B7 in Fig. 1) and backup outlets along the coast when the city's sewerage system overflows (personal communication with the city water authority, AcuaCar).

The bay's seasonal conditions may be categorized by the variability of winds, freshwater discharge and water quality. The Dique Canal's highest discharges typically occur from October to December, while its lowest levels occur from February to April. Winds are strongest and predominantly northerly from January to April due to the trade winds which coincide with the strengthening of the southern Caribbean upwelling system and the cooling of water temperatures (Andrade and Barton, 2005; Lonin et al., 2004; Rueda-Roa and Muller-Karger, 2013). Breezy conditions are observed from August to November, when weaker winds come from highly variable directions. Tosic et al. (2019) demonstrated the seasonal variability of the bay's water quality between the rainy season (Sept.–Dec.) when the waters are characterized by lower salinities and greater concentrations of suspended sediments, nutrients, and pathogenic bacteria; the windy season (Jan.–Apr.) which produces lower water temperatures and greater levels of organic matter; and the transitional season (May–Aug.) when the highest temperatures and lowest levels of dissolved oxygen are found.

2.2. Data collection

Bathymetric data with 0.1 m vertical resolution were digitized from georeferenced nautical maps (#261, 263, 264) published by the Colombian Navy's Center for Oceanographic and Hydrographic Research (CIOH-DIMAR). In the 3 × 2 km area of Bocachica strait, the digitized bathymetry was updated with high-precision (1 cm) bathymetric data collected in the field on 17 Nov. 2016. Depth was measured along 30 transects perpendicular to the navigation canal using a GPS-linked Knudsen 200 kHz mono-beam echo-sounder mounted on the side of a boat.

Water quality was monitored monthly in the field from Sept. 2014 to Nov. 2016 between the hours of 9:00–12:00 (Karydis and Kitsiou, 2013). Measurements were taken from 9 stations (Fig. 1), including one station in the Dique Canal (C0) and eight stations in Cartagena Bay (B1-8). At all stations, CTD casts were deployed using a YSI Castaway measuring salinity and temperature every 30 cm of depth. Grab samples were taken from surface waters and analyzed at the nearby CARDIQUE Laboratory for total suspended solids and chlorophyll-*a* by standard methods (APHA, 1985). A Secchi disc was also deployed to measure water transparency while a Kestrel 4500 Pocket Weather Tracker was used for *in situ* measurements of winds, air temperature, and relative humidity. Crude observations of cloud cover were also recorded. At station C0 in the Dique Canal, water velocity was measured with a Sontek mini-ADP (1.5 MHz) along a cross-stream transect three times per sampling date and discharge values were subsequently calculated with the Sontek River Surveyor software.

CTD data were used to calculate the Brunt–Väisälä frequency, or

buoyancy frequency, along the water column. The Brunt–Väisälä frequency (N) computes the natural frequency of oscillation of a water parcel given a small vertical displacement from its equilibrium position using the following equation: $N = \sqrt{-(\frac{\partial \rho}{\partial z} \bullet \frac{g}{\rho_0})}$, where $\frac{\partial \rho}{\partial z}$ represents the vertical density gradient, g is the acceleration due to gravity, and ρ_0 is the *in situ* density (Pingree & Morrison, 1973).

Hourly METAR data of wind speed, wind direction, air temperature and relative humidity were obtained from station SKCG at Rafael Núñez International Airport (approximately 10 km north of the bay; Fig. 1). Albedo, cloud cover, and precipitation data were obtained at a location 3 km offshore of Cartagena Bay from datasets available from NOAA's Global Forecast System (GFS) with 3-h frequency. Daily profiles of temperature and salinity were obtained from the European Union's Mercator Ocean Model at a location 10 km offshore of the bay. Tidal components were obtained for numerous locations offshore of the bay from the finite element solution tide model FES2004 (Lyard et al., 2006) using the MOHID Studio software. Hourly measurements of water levels at a location within the bay (Fig. 1) were also obtained from the Colombian Navy's Center for Oceanographic and Hydrographic Research (CIOH-DIMAR).

2.3. Model application

The flow regime of Cartagena Bay was simulated using the MOHID Water Modelling System (Leitão et al., 2008; Mateus and Neves, 2013). The MOHID Water model is a 3D free surface model with complete thermodynamics along with eulerian and lagrangian transport models. MOHID is based on the finite volume approach and calculates hydrodynamic fields based on the solution of the Reynolds equations of motion, assuming hydrostatic balance and the Boussinesq approximation. The model utilizes an Arakawa C grid for its horizontal discretization which computes scalars at the center of each cell and vectors at the face of each cell. It also implements a semi-implicit time-step integration scheme and permits combinations of Cartesian and sigma coordinates for its vertical discretization (Martins et al., 2001). Vertical turbulence is computed by coupling MOHID with the General Ocean Turbulence Model (GOTM), which consists of a generic library with several different turbulence closure schemes for the parameterization of vertical turbulent fluxes in marine waters (Burchard, 2002). In this work, a scheme similar to a two equation K-epsilon solution is used, corresponding to level 2.5 of the Mellor & Yamada classification.

Model configuration for Cartagena Bay was based on an equally-spaced Cartesian horizontal grid with a resolution of 75 m and a domain area of 196 km^2 (Fig. 1). This included an offshore area 2.3 km outside the bay, though only the results inside the bay are considered within the limits of the monitoring stations used for calibration. A mixed vertical discretization of 22 layers was used by incorporating a 7-layer sigma domain for the top five meters of depth and a variably-spaced (depth-incrementing) Cartesian domain below that depth. Depths within the bay were covered by 18 of the 22 vertical layers, while the bottom four layers covered the greater depths outside the bay. This was possible due to the generic vertical geometry of MOHID and was chosen to reproduce the mixing processes of the highly stratified bay. Given these defined dimensions, the MOHID Studio software was used to generate a bathymetric grid based on the digitized nautical maps that were updated with field-measurements in the area of Bocachica strait.

The model includes the main factors determining the circulation within the bay. The horizontal density gradients occurring within the bay are influenced by the freshwater input of the Dique Canal, the tide-driven input of seawater at the model domain's open boundary, and atmospheric fluxes of heat (solar radiation, longwave radiation, latent heat and sensible heat) and water (precipitation, evaporation) at the bay's surface. The gradient of water level is influenced by lateral tidal forcing and elevated water levels created by freshwater accumulation and wind-driven “pile-up”. The horizontal gradient of atmospheric pressure is ignored. The Coriolis force is considered, though its effect is minimal in this case given the low latitude of 10°20′ N. Wind stress is applied to the surface layer as a boundary condition.

Open boundary conditions were imposed by prescribing values based on reference solutions (Dirichlet boundary conditions). The lateral forcing of the tides was determined by the harmonic components extracted from the FES2004 model at numerous locations along the boundary. Daily profiles of seawater temperature and salinity extracted from the Mercator model were imposed at the open sea boundary. Measured monthly values of discharge and velocity for the inflowing Dique Canal were imposed as a time series from which the model interpolates values of water flow and momentum for each time step during the simulation period. Atmospheric variables were all prescribed as spatially-constant fields with frequencies of 1-h (METAR data: wind velocity, air temperature, relative humidity) or 3-h (GFS data: albedo, cloud cover, precipitation data). These meteorological datasets were compared with field observations for verification. The evaporation rate and heat fluxes (solar and non-solar radiation) at the bay's surface were calculated by the model.

Given the importance of surface water transparency on short-wave radiation penetration and the resulting heat flux, multiple calculation methods of the short-wave light extinction coefficient (K_d) were compared utilizing the field measurements of total suspended solids (TSS), chlorophyll-*a* and Secchi depth. These included previously established relationships between K_d-TSS and K_d-Secchi in Cartagena Bay (Lonin, 1997a), K_d-TSS and K_d-Secchi relationships in coastal and offshore waters around the United Kingdom (Devlin et al., 2008), a relationship for K_d-chlorophyll-*a* in oceanic waters (Parsons et al., 1984), a K_d-TSS relationship developed for the Tagus estuary, Portugal (Portela, 1996), and a combined K_d-TSS-chlorophyll-*a* relationship based on Portela (1996) and Parsons et al. (1984). The K_d-TSS relationship of Portela (1996) was finally selected for use in this study as model simulations using these K_d values produced thermoclines most similar to field observations.

Three simulation periods of a lunar-month duration in the year 2016 were focused on for the present modelling study, each considered representative of distinct seasonal conditions in the bay (Tosic et al., 2019): the windy season (27 Jan. – 24 Feb.), the transitional season (28 June – 26 July), and the rainy season (19 Oct. – 17 Nov.). Start and end times for each simulation coincided with the dates of monthly field sessions. After testing various time steps, an optimal Δt of 20 s was chosen. Initial conditions of water temperature and salinity were defined as vertical profiles based on CTD measurements made on the corresponding start date. To avert numerical instabilities, a spin-up period of one day was applied to gradually impose wind stress and open boundary forcings (Franz et al., 2016).

Outputs from the simulations were then processed, analyzed and compared with field measurements. Each simulation's final water temperature and salinity were extracted as profiles at each sampling station location (B1-B8; Fig. 1) and compared to the CTD measurements of the respective end date. Measurements from the CIOH tidal gauge were compared to hourly time series of water height extracted from each simulation's output at the gauge's location (Fig. 1). Instantaneous and mean water velocity fields and water heights were also analyzed from each simulation's output.

To evaluate model performance, various descriptive statistics were calculated to compare the simulated (predicted: P) and measured (observed: O) values of water temperature, salinity and water height. Being N_s the sample size, these included the mean of observed ($\bar{O}$) and predicted ($\bar{P}$) values, and the sample standard deviation of observed (s_O) and predicted (s_P) values (Willmott, 1982). The average error ($AE = \Sigma(P_i - O_i)/N_s$) was calculated as a measure of aggregate model bias in order to identify the model's tendency to over- or under-estimate observed values, while keeping in mind that positive and negative discrepancies can cancel one another (Zhang and Arhonditsis, 2008). The magnitude of the model's prediction accuracy is shown by the mean

absolute error (MAE = $\Sigma|P_i - O_i|/N_s$)) and the root mean squared error (RMSE = $(\Sigma(P_i - O_i)^2/N_s)^{0.5}$), the latter of which is sensitive to the inaccuracies of outliers (Willmott and Matsuura, 2005). The relative error (RE = $\Sigma|P_i - O_i|/\Sigma O_i$) was also calculated in order to express error as a percentage of the observed values (Arhonditsis and Brett, 2004), noting that this measure is dependent on the magnitude of the variable itself.

Model calibration and validation were based on the analysis of the aforementioned statistics for each of the three simulations. The rainy season simulation was utilized for calibration, while the windy and transitional season simulations were used for validation. In order to select calibration parameters, a sensitivity analysis was carried out to assess the influence of parameters with uncertain values on model results. Simulations were run in which each of the following parameters were reduced by one half and increased two-fold (Arhonditsis et al., 2000): horizontal viscosity, surface water roughness and bottom roughness. Additionally, two other horizontal advection methods were tested: 2nd order upwind and Total Variation Diminishing. The effect that each parameter modification had on the salinity, temperature and water level (quantified by the aforementioned statistics) was then compiled and compared to determine the most important parameters for model calibration. Horizontal viscosity and bottom roughness (used to compute the drag coefficient) were ultimately selected as calibration parameters, yielding final calibrated values of 12.0 m^2/s and 0.006, respectively.

A Lagrangian approach was used to compute residence times and flushing times of the water in Cartagena Bay during the different seasonal simulations (Braunschweig et al., 2003). MOHID's Lagrangian transport model was used to trace the evolution of passive particles emitted at slack water tide from two origins: 1) the Dique Canal and 2) throughout the bay itself. To assess the residence times of canal water in the bay, a total of 1080 particles were emitted from the canal over a period of six hours. To assess the residence time and flushing time of the full volume of water in the bay, another 320,657 particles were instantaneously emitted throughout all areas and depths of the bay (1 particle per cell). Both particle emissions were set to occur four days following the start of the simulation in order to postpone particle evolution until after the initial phase of hydrodynamic stabilization. Monitoring boxes set up in the model tracked the total volume of particles during the simulation in three layers: the surface (top 5 m of depth), mid-layer (5–14 m depth) and bottom layer (14–32 m depth). Given the probability that a few particles may become trapped in small inlets within the bay, for practical purposes flushing time was defined as the time necessary for 95% of the particles to flush out of the bay (Jouon et al., 2006). As the particles emitted throughout the bay (origin 2) did not meet this 95% criteria within the time period of the simulations, exponential curves were fitted to the particle evolution trend in order to calculate the bay's flushing time (Monsen et al., 2003). These curves were also used to estimate a mean residence time for the bay's water given as τ in the exponential equation: $m(t) = m(0)\exp(-t/\tau)$, which is the time at which the volume of tracers is reduced to approximately 36.8% ($1/e$) of its initial volume (Braunschweig et al., 2003). This methodology was chosen to evaluate the magnitude and importance of both seawater renewal and vertical exchanges in the bay.

Additionally, numerical experiments were carried out with the model to evaluate two hypothetical scenarios. The first scenario consisted of doubling the freshwater discharge from the Dique Canal in consideration of hydrological trends projecting significant future increases in runoff associated with watershed deforestation and climate change (Restrepo et al., 2016). The other scenario entailed halving the canal's discharge in order to reflect the reduced flow planned by the ongoing hydraulic intervention, which proposes to construct hydraulic doors along the canal (Fondo Adaptación, 2018). For each of the six numerical experiments (two scenarios, three simulated seasons), residence and flushing times were calculated using the Lagrangian approach and water velocity fields were analyzed in order to evaluate the simulated impact on the bay's hydrodynamics.

3. Results

3.1. Monitoring results

Over the 27-monthly monitoring sessions, salinity, temperature and density in the bay ranged from 0 to 36.5, 26.7–33.2 °C and 995.9–1023.6 kg/m^3, respectively. The bay's minimum values of salinity and density were found at the surface of the Dique Canal outlet from Oct.–Dec. 2014. Maximum temperatures were found at the surface of station B5 in Oct. 2015. Among surface waters, the maximum salinity (35.8), minimum temperature (27.6 °C) and maximum density (1022.8 kg/m^3) values were found at station B8 (Bocagrande) in Jan. 2015. Bottom waters were much more homogenous horizontally, with multiple stations presenting the maximum density and salinity values in April and May, respectively, of 2016. Measurements in bottom waters yielded minimum values of salinity (35.3) and density (1022.1 kg/m3), along with maximum temperature (29.2 °C) at multiple stations in Nov. 2016. Overall minimum temperatures were found in the bay's bottom waters in March 2015.

Excluding the Dique Canal outlet itself, only minor horizontal spatial variation is observed among the different locations (B1-8) of Cartagena Bay (Fig. 2). A greater influence of freshwater, in terms of lower salinity, density and higher temperature, was found at stations B4 and B5 in front of the Dique Canal. Conversely, a stronger influence of marine water was seen at the furthest station (B8) from the canal.

Temporal and vertical spatial variations were remarkably pronounced at all stations. Graphical visualizations are focused on the results of station B5 (Fig. 3) which exhibited slightly more variability than the other stations due to the canal's proximal freshwater influence. Well-defined seasonal conditions were observed with vertically mixed marine conditions during the windy season (Jan.–April) and highly stratified gradients of salinity and temperature in the rainy (Sept.–Nov.) and transitional (May–Aug.) seasons, respectively.

Inter-annual variation was also apparent, reflecting the influence of the El Niño phenomena of 2015, when reduced precipitation and runoff resulted in higher temperatures and salinities in the bay. Of particular note are the surface temperatures occurring between Aug.–Oct. 2015 (31.5–33.2 °C) which were greater than the corresponding months in 2014 and 2016 (avg. 30.8 ± 0.2 °C). The effect of less runoff during 2015 is also visible in the vertical salinity gradients, as the rainy season influence of freshwater during Sept.–Oct. 2014 and Oct.–Nov.2016 reaches greater depths than in the 2015 rainy season.

The effects of surface heating and water mass fluxes can be distinctly observed in the vertical density profiles. Temporal variation of surface heating, particularly between April and October 2015 but also from May to July 2016, results in greater vertical density gradients and lower bottom densities. Abundant freshwater surface fluxes between September and November have a similar effect along the vertical density gradient, though the influence of freshwater can also be seen in the salinity and density of surface waters in April and May.

The seasonal variation of vertical mixing is well-pronounced as less thermohaline stratification is observed between January and March. This is due to increased wind speeds during this season as well as to the effect that decreased freshwater input has on reducing the pycnocline, which in turn allows wind-generated turbulence at the surface to penetrate lower depths. Cooler bottom waters are also likely related to the strengthening of the southern Caribbean upwelling system (Andrade and Barton, 2005; Rueda-Roa and Muller-Karger, 2013). The overall effect of this thermohaline variation results in the bay's water density gradually decreasing from April to November and then in December sharply reverting to conditions more similar to seawater.

There also appears to be a time-lag between surface and bottom effects. For example, decreased surface densities in May and October, caused by freshwater runoff, are not transferred to the bottom waters

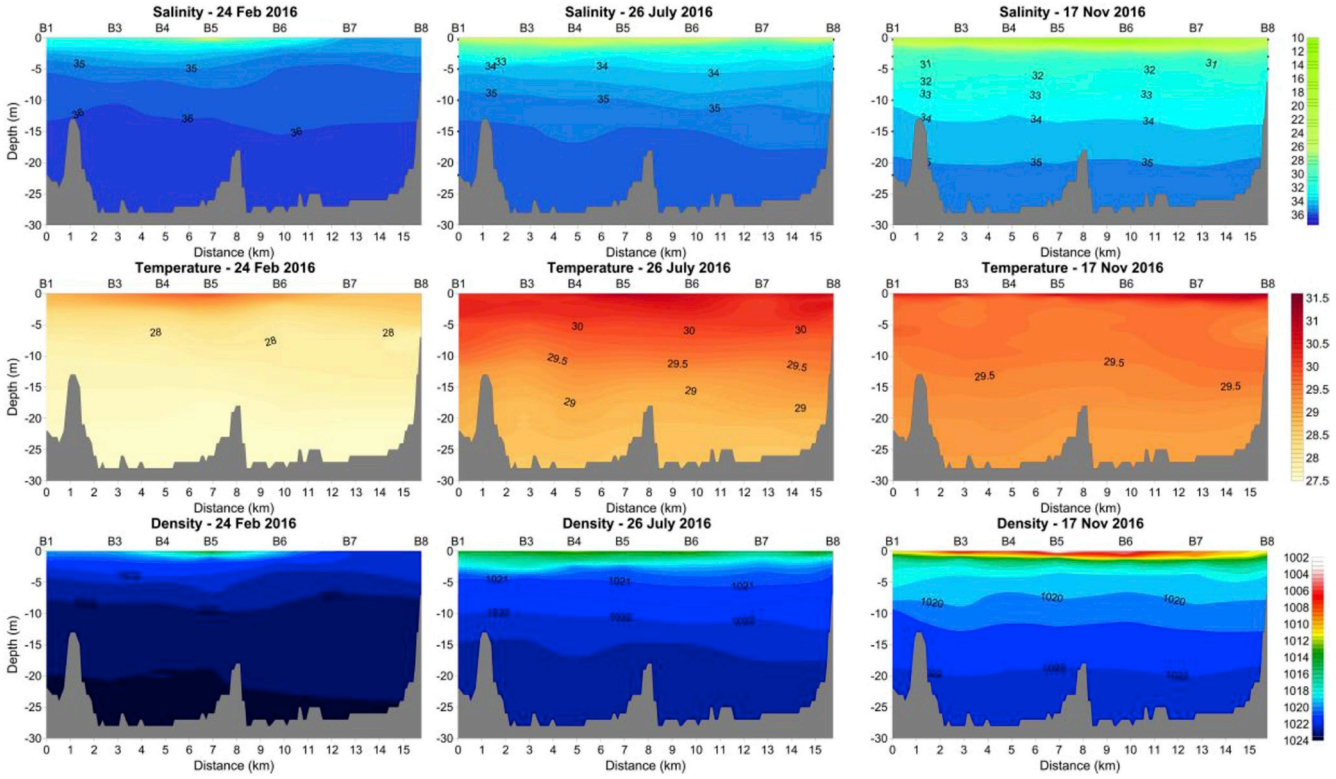

Fig. 2. Vertical profiles of salinity (top), temperature (middle) and density (bottom) measured during the windy (24-Feb; left), transition (26-July; center) and rainy (17-Nov; right) seasons of 2016 and horizontally interpolated between sampling stations (B1-8).

until June and November, respectively. This is reflective of the time required for vertical mixing and the impeding effect of strong vertical stratification.

Brunt–Väisälä frequencies further illustrate the processes of vertical mixing (Fig. 3d). Higher frequencies are indicative of steeper density gradients where there is resistance to vertical mixing, while lower frequencies are characteristic of a stratification closer to neutral, facilitating the vertical displacement of turbulent eddies and increasing the efficiency of vertical mixing.

Measurements between Sept. 2014 and Nov. 2016 revealed greater Brunt–Väisälä frequencies in surface layers (Fig. 3d). Lower frequencies below 1 m depth from Jan.–Apr. 2016 demonstrate the greater potential for vertical mixing during the windy season. Maximum frequencies were typically found within the top 1 m of surface water with the exception of Feb. and Sept. 2015 when maxima were found 1.5 and 2.5 m depths, respectively. In Feb. 2015, the depth of this maximum value may be a reflection of reduced freshwater input and greater vertical mixing during this month which led to higher salinities being found at the surface. In contrast, the deeper maximum value found in Sept. 2015 could be a result of fluxes of heat and freshwater which penetrated deeper below the surface than usual (Fig. 3a and b), producing a homogeneously mixed surface layer, a corresponding frequency minimum near the surface, and the vertical displacement of the pycnocline down to 2.5 m depth.

3.2. Model performance

The calibrated model adequately reproduced field observations of temperature, salinity and water level, as shown by the different performance statistics analyzed (Table 1), indicating that the model effectively simulates the hydrodynamics of the system. Mean values of temperature, salinity and water level observed during the three simulation months were in close agreement with mean values produced by the model, yielding differences of 0.05–0.26 °C and 0.15–0.53 in temperature and salinity, respectively, and just a 1 mm difference in mean water levels. Similar standard deviations between observed and predicted values show that the model captured the observed spatio-temporal variation. The standard deviations of observed data were consistently slightly greater than the standard deviations of modelled values. This may be expected due to the variety of factors in the natural environment which can generate additional variability (e.g. waves, storms, urban wastewater) that are not considered in the model.

Hourly observations of water level were in very close agreement with those generated by the model (Appendix A). Despite the occurrence of periods with missing observational data, calibration of the mean water level allowed for closely corresponding tidal oscillation in the model results. Small differences between observed and modelled water levels were prevalent at peaks of high- and low-tides. Nevertheless, values of MAE (0.031–0.039 m) and RMSE (0.039–0.048 m) were quite low, suggesting that these differences were of minimal consequence. While values of RE may appear high (8.8–11.4%), this is relative to the small magnitude of water levels in general.

Temperature profile observations were particularly well reproduced by the model in the rainy and windy season simulations (Appendix A), which yielded MAE and RMSE values of 0.20–0.21 °C and 0.28–0.29 °C, respectively. The transitional season simulation produced slightly higher values of 0.36 °C and 0.39 °C, respectively, which may be a result of this season having a more dynamic thermal structure as it also yielded the highest mean (29.85 °C) and standard deviation (0.52 °C) of observed temperatures. In general, the model showed an overall bias of

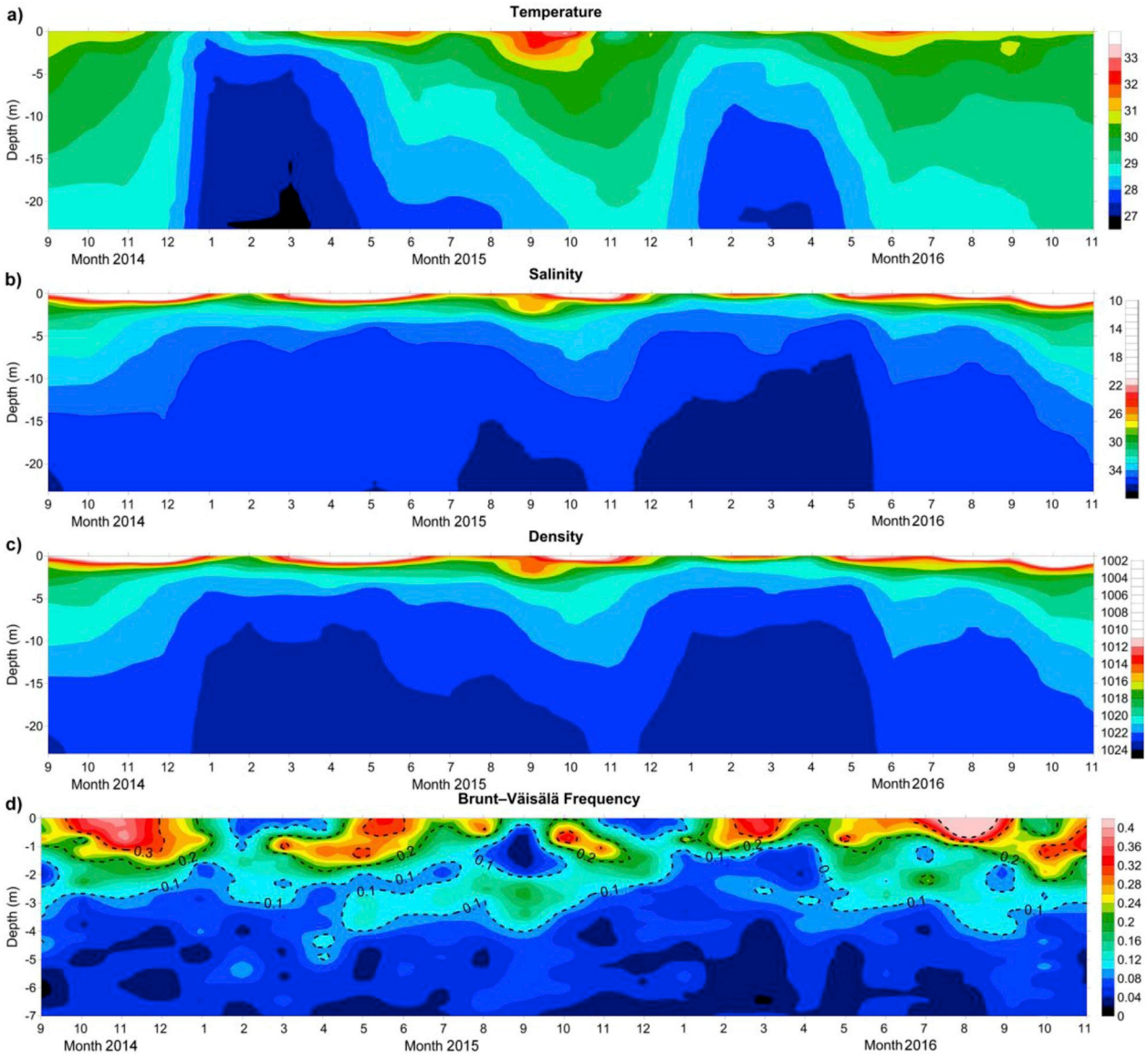

Fig. 3. Hovmöller diagrams of vertical profiles of temperature (a), salinity (b) and density (c) measured at station B5 during 27 monthly sampling sessions (Sept. 2014–Nov. 2016) and interpolated over time. Calculations of the Brunt-Väisälä frequency (d) are shown for the top 7 m of surface water.

underestimating temperatures as AE values were all negative (Table 1). However, the plots of observed and predicted temperature profiles (Appendix A) show that this underestimation commonly occurred at shallower depths, while temperature at deeper depths was usually overestimated. Therefore, the model produced temperature profiles that were less vertically stratified than in the observed profiles. Regardless, the low values of MAE, RMSE, and RE (0.7–1.2%) showed that temperature was adequately reproduced by the model, especially

Table 1
Statistics of model performance: sample size (N_s), mean and standard deviation of observed ($\bar{O}$, s_O) and predicted ($\bar{P}$, s_p) values, average error (AE), mean absolute error (MAE), root mean squared error (RMSE), and relative error (RE).

Parameter	Season	*Ns*	$\bar{O}$,	$\bar{P}$	s_O	s_P	AE	MAE	RMSE	RE
Temperature (°C)	Rainy	108	29.62	29.57	0.26	0.18	−0.05	0.21	0.28	0.7%
	Tran	108	29.85	29.59	0.52	0.30	−0.26	0.36	0.39	1.2%
	Dry	108	28.23	28.05	0.49	0.32	−0.17	0.20	0.29	0.7%
Salinity	Rainy	108	30.54	31.03	4.49	3.71	0.49	1.36	2.13	4.5%
	Tran	108	33.04	32.89	2.83	2.82	−0.15	0.80	1.09	2.4%
	Dry	108	34.99	35.52	1.40	0.62	0.53	0.60	1.03	1.7%
Water Level (m)	Rainy	496	0.390	0.386	0.112	0.092	−0.001	0.034	0.044	8.8%
	Tran	625	0.284	0.283	0.110	0.094	−0.001	0.031	0.039	10.9%
	Dry	277	0.338	0.342	0.097	0.092	0.001	0.039	0.048	11.4%

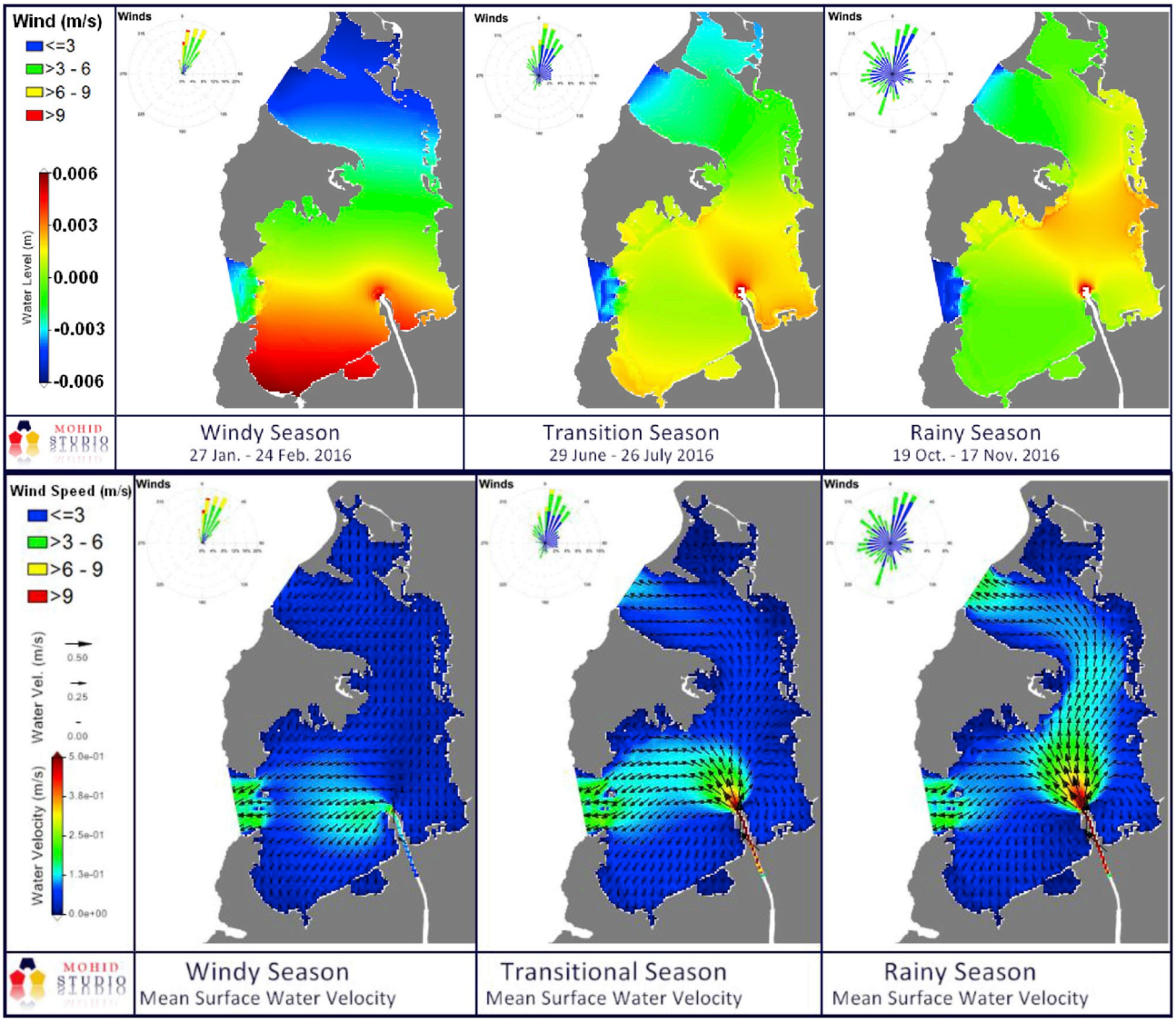

Fig. 4. Mean water level (above), mean surface water velocities (below) and wind roses during simulations of the windy (left), transition (center) and rainy (right) seasons of 2016.

considering that the model's vertical resolution (71–78 cm at the surface, depending on the tide) cannot completely reproduce the strong vertical gradients at the surface.

Predicted salinity profiles produced higher RE values (1.7–4.5%) than those of temperature profiles. However, visual comparison of the predicted and observed salinity profiles (Appendix A) suggest that the model was quite effective in simulating the bay's haline stratification, as modelled salinity profiles were very similar to observations. The principal source of error can be seen to occur at the surface where observed salinities are occasionally much lower than predicted values. This overestimation in surface water salinity is to be expected given that various additional sources of freshwater input are not included in the model, such as urban runoff and local sources of domestic and industrial wastewater. This discrepancy is reflected in values of RMSE, a statistic which tends to amplify the effect of outliers, yielding greater error in the rainy season (2.13) than in the other two season (1.03–1.09).

3.3. Hydrodynamic modelling results

The mean water levels during each simulation showed slight spatial variation across the bay with differences of approximately 1.2 cm (Fig. 4). The most pronounced variation of mean water level was observed during the windy season simulation when strong northerly winds generated a north-south gradient with higher mean water levels at the southern end of the bay than at the northern end. The rainy season simulation resulted in higher mean water levels in the central part of the bay due to the accumulation of freshwater discharge from the Dique Canal. Meanwhile, during the transitional season, a combined effect is observed with elevated water levels found both around the Dique Canal's outlet area and in the bay's southern end. Seasonal variability was also observed as mean water levels were greatest in the rainy season (38.0–39.2 cm), followed by the windy season (34.1–35.3 cm) and lowest during the transitional season (27.9–29.1 cm) with respect to the mean lower low water (MLLW).

Mean surface water velocities during the three seasonal simulations (Fig. 4) exhibit the dominant influence of discharge from the Dique Canal on the bay's surface currents. At high (rainy season) and medium (transitional season) discharge levels, the Dique Canal forces surface currents to run north and west to the two seaward straits. Mean surface currents during the transitional season are stronger in the westward direction and weaker in the northward direction as a result of winds coming predominantly from the north. During the windy season, strong northerly winds overpower the low discharge levels and force mean

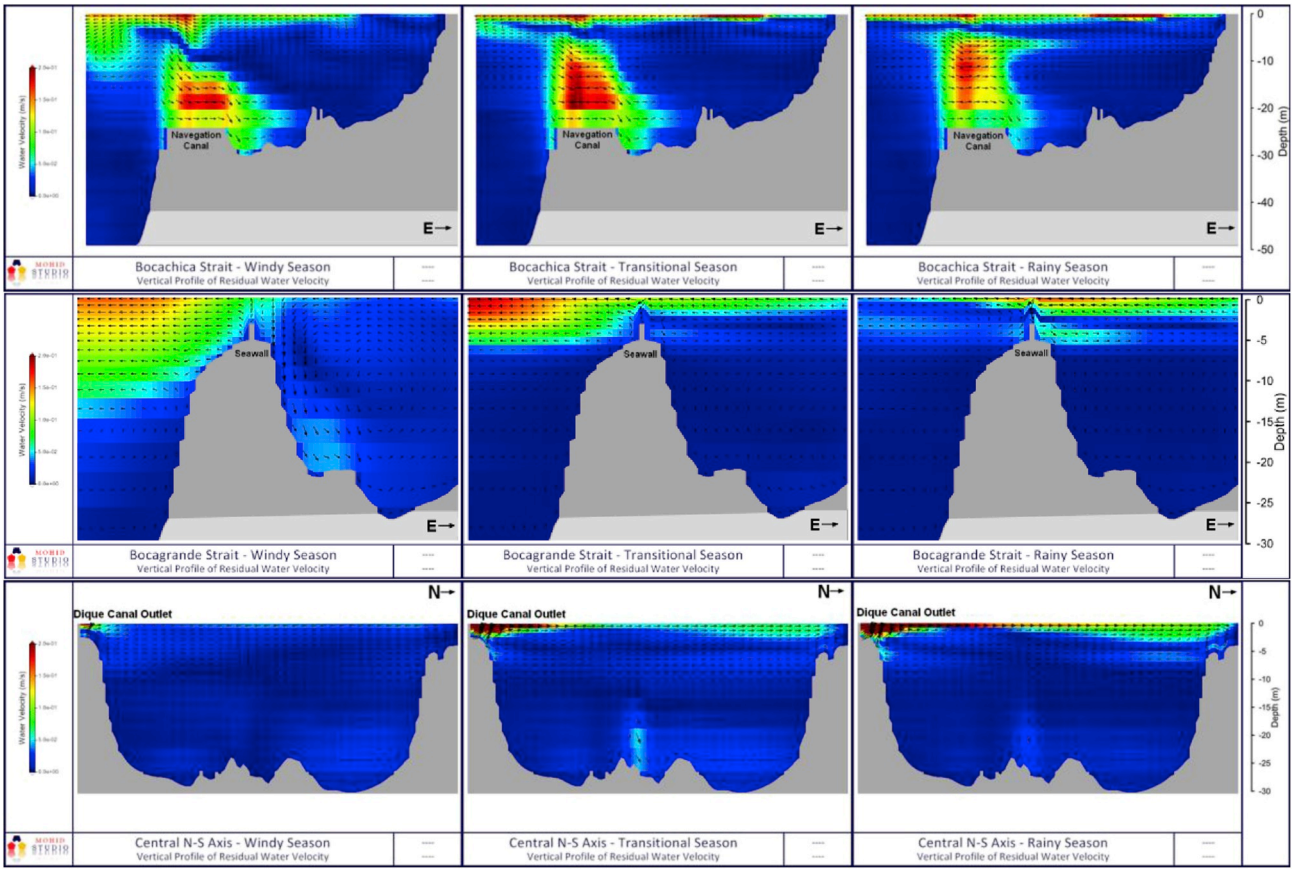

Fig. 5. Vertical profiles of mean water velocities along the latitudes of the Bocachica navigation canal (above), Bocagrande strait (middle) and along the longitude of the Dique Canal outlet and central part of the bay (below) for simulations of the windy (left), transition (center) and rainy (right) seasons. See Fig. 1 for locations of profiles.

surface currents throughout the bay in a southwest direction. The effect of windy season conditions on the bay's seaward outflow can be seen as mean surface currents flow out of the southern strait, Bocachica, but appear to flow parallel to the seawall in the northern strait, Bocagrande, resulting in reduced seaward exchange and recirculation of bay water.

Vertical profiles of mean water velocities during the three simulations illustrate some of the bay's processes of circulation and water exchange with the sea (Fig. 5). In all cases, the pronounced vertical stratification generates distinct surface and sub-surface currents that form the estuary's gravitational circulation. At Bocachica strait (Fig. 5, top), freshwater flows out from the bay at the surface, while seawater flows in via the navigation canal below. While these currents in the rainy and transitional season simulations are quite similar, the stronger westward surface velocities during the transitional season result in higher velocities flowing into the bay in the bottom depths of the navigation canal. During the windy season simulation, outflowing currents run deeper into the navigation canal (0–6 m depths) than in the other two seasons (0–3 m depths), resulting in a deepening of the inflowing seawater current as well. This deepening of outflowing water may be expected during the windy season given that thermohaline stratification is reduced and that mean surface outflow was concentrated through Bocachica (Fig. 4).

At Bocagrande strait (Fig. 5, middle), outflowing surface water and inflowing sub-surface water were also observed, though the latter was inhibited by the sub-surface seawall. Again the currents in the rainy and transitional season simulations were quite similar, though in this case the stronger northward surface velocities during the rainy season (Fig. 4) were balanced by faster sub-surface inflow atop the seawall. Velocity fields during the windy season are quite different as little inflow or outflow is observed over the seawall (Fig. 5); but rather, surface currents plunge downwards on the inner side of the seawall and create a vertical circulation cell.

Distinct windy season currents were also evident in vertical velocity profiles along the north-south central axis of the bay (Fig. 5, bottom). During the windy season, surface currents ran southwards and two sub-surface vertical circulation patterns are observed in opposite directions: one in the north part of the bay at a depth of approximately 5 m and another in the south part of the bay at approximately 8 m depth. During the rainy and transitional seasons, northward surface currents were balanced by southward sub-surface currents, though in the case of the transitional season this sub-surface current was slightly deeper than during the rainy season. Mean bottom currents ran northwards during the rainy and transitional seasons, and southwards during the windy season. A distinct column of upward and downward vertical exchange in the center of the bay was detected in the rainy and transitional seasons (Fig. 5).

Mean water velocities revealed a sub-surface horizontal eddy in the southwest part of the bay. At 2.5 m depth, this eddy flowed counter-clockwise during all three seasons as the northern part of the eddy contributed to the surface outflow at Bocachica. At 5.5 m depth, the eddy was reversed to a clockwise circulation pattern during the rainy and transitional season, as the northern part of the eddy corresponded

to seawater inflow through Bocachica at this depth. However, during the windy season, the deepening of the surface outflow at Bocachica also resulted in a deepening of the counter-clockwise eddy which was maintained at 5.5 m depth, while the clockwise eddy was found at deeper depths of approximately 10 m.

Deviations from mean water velocities were exhibited by instantaneous water velocity fields. The direction of instantaneous surface velocities during the rainy and transitional seasons occasionally varied when moderate winds came from the north or west in opposition to the northward and westward flowing surface waters, though velocities around the Dique Canal outlet were consistently in a north-northwest direction. Instantaneous surface velocities in the two straits during the rainy and transitional seasons were consistently in a seaward direction and only rarely changed direction when flood tides coincided with moderate westerly winds. In the windy season, instantaneous surface water velocities typically followed the wind direction throughout the bay, including the Dique Canal outlet area, but with the exception of the Bocachica strait where a seaward surface outflow was maintained.

The effect of tidal currents was clearly observed in vertical profiles of instantaneous velocities in Bocachica strait where the speeds at all depths and direction at sub-surface depths (3–5 m) oscillated with the tides in all three seasonal simulations. During flood tides, bottom waters flowing into the bay increased in speed and occupied a greater proportion of the navigation canal's water column. Ebb tides resulted in increased speeds of outflowing surface waters that extended to deeper depths of the water column. Occasionally, a layer of outflow was also observed at bottom depths of the navigation canal during the rainy and transitional seasons. In the windy season, a vertical eddy was sometimes observed in the navigation canal between the layers of surface outflow and sub-surface inflow.

A similar tidal oscillation was observed in the instantaneous velocities in Bocagrande strait. In the rainy and transitional seasons, surface water outflow intensified during ebb tides. Occasionally, the intensified surface outflow during ebb tides in the rainy season dominated water exchange in the strait such that outflowing currents were observed at all depths. During flood tides, sub-surface inflow intensified in the rainy season, though in the transitional season, sub-surface currents atop the seawall were characterized by the downwelling and recirculation of surface waters. During the windy season, the vertical circulation cell found in mean water velocities on the inner side of Bocagrande (Fig. 5) was maintained throughout nearly the entire simulation, while the waters atop the seawall oscillated between inflow and outflow at all depths uniformly.

Along the north-south central axis of the bay, vertical profiles of instantaneous water velocities (Fig. 6) were very different from mean water velocities during the windy season. While mean water velocities portrayed a velocity field characterized by low speeds (Fig. 5, bottom), instantaneous water velocity fields revealed fluctuating hydrodynamics with high speeds. Numerous vertical circulation cells were frequently observed at varying locations while current directions changed often. A column of upward and downward vertical exchange in bay's center was also detected, similar to that of mean water velocities during the rainy and transitional seasons.

3.4. Water renewal time scales

Under the present conditions, the mean residence time of particle tracers emitted from the Dique Canal varied between 3 and 6 days, while their flushing time ranged from 10 to 20 days (Table 2). During the rainy and transition seasons, particles were transported north due to the canal's influence, though their extension was slightly reduced during the transition season due to lower discharge and stronger wind (Fig. 7). In the windy season, intense northerly winds confined particles in the southern lobe of the bay. The shorter residence time of canal water during the rainy season (2.7 ± 4.2 days) is reflective of the greater surface water velocities resulting from the high discharge and weak variable winds of the rainy season (Fig. 4). The constraining effect of the wind was particularly apparent in the flushing time of the windy season (19.9 days) when compared to the shorter flushing times of transitional (13.2) and rainy (10.2) seasons.

For particle tracers emitted throughout the bay's complete volume of water, the mean residence time varied between 23 and 33 days while the overall flushing time ranged from 70 to 99 days. In this case, the residence (32 days) and flushing times (97–99 days) of the rainy and transitional seasons were quite similar (Table 2). However, the shorter time scales during the windy season are indicative of the increased vertical mixing during this season bringing particles from lower depths up to the surface where they can flow out of the seaward straits. Processes of vertical exchange and the shorter flushing time during the windy season are evident in Fig. 8, illustrating the oscillation of particles between surface and sub-surface depths in unison with the tides.

Under scenarios of increased or decreased discharge conditions, water renewal time scales were greatly affected in most cases. Doubling the Dique Canal's discharge substantially reduced the residence and flushing times of particles emitted throughout the bay in all three seasons. A similar effect was observed on the water renewal time scales of canal particles during the rainy and transitional season. While a reduction in water renewal time scales under double-discharge conditions also occurred during the windy season, the effect was less significant.

By halving the canal discharge, water renewal time scales nearly doubled under rainy season conditions. This scenario also increased

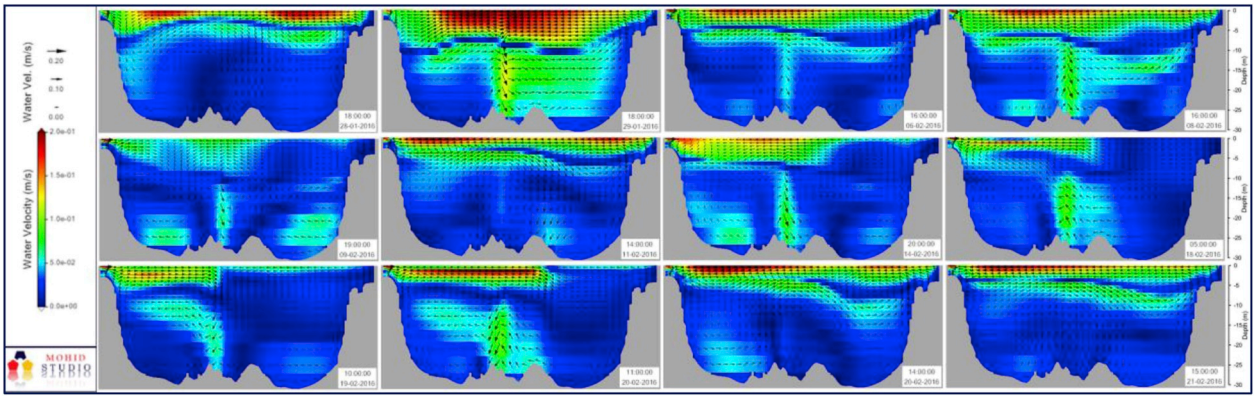

Fig. 6. Snapshots of vertical profiles of instantaneous water velocities along the longitude of the Dique Canal outlet and central part of the bay (see Fig. 1 for location) during the windy season simulation. The Dique Canal outlet is to the left and north is to the right.

Table 2
Mean residence times (± standard deviation) and flushing times (in days) of particles emitted from the Dique Canal and the entire bay during three seasons under three scenarios: the present, double-discharge (Qx2) and half-discharge (Qx0.5) of water from the Dique Canal. Environmental parameters of canal mean discharge values (m^3/s) along with mean wind speed (m/s) and direction (°) are also presented.

	Rainy Season			Transition Season			Windy Season		
	Present	Qx2	Qx0.5	Present	Qx2	Qx0.5	Present	Qx2	Qx0.5
Environmental Parameters									
Mean Canal Discharge (m^3/s)	225.0	450.0	112.5	167.3	334.7	83.7	33.9	67.7	16.9
Mean Wind (m/s) & Dir. (°)	3.0 (309°)			3.3 (10.3°)			5.0 (16.6°)		
Canal Emission									
Mean (± St.Dev.) Residence Time (d)	2.7 ± 4.2	1.8 ± 2.5	5.6 ± 4.6	5.0 ± 4.2	2.8 ± 2.2	7.6 ± 4.9	5.7 ± 4.6	5.6 ± 4.4	3.8 ± 5.1
Flushing Time (d)	10.2	5.0	18.8	13.2	7.5	21.7	19.9	16.9	18.2
Bay Emission									
Mean Residence Time (d)	32.5	11.7	56.3	32.2	22.6	36.5	23.1	12.2	23.7
Flushing Time (d)	98.5	34.8	171.8	97.3	68.8	113.4	70.2	35.3	69.9

time scales during the transitional season, though not as much as during the rainy season. However, halving the canal discharge did not increase time scales during the windy season, but rather, had the effect of slightly decreasing the time scales of canal particles and had relatively no effect on the particles emitted throughout the bay.

Overall, by doubling the freshwater discharge, the bay's flushing times were reduced and there was less variation between the seasons (Fig. 8). Conversely, halving the freshwater discharge resulted in increased flushing times, with exception to the windy season, and greater variation between the seasons. A clear relationship was observed between discharge and flushing time of canal water yielding an exponential trend line with an R^2 value of 0.939 (Fig. 9). Discharge-dependent relationships were less pronounced for canal water residence time as well as bay water residence and flushing time due to the exceptions occurring under windy, low-discharge conditions. However, by grouping results of only the rainy and transitional seasons, clear exponential relationships can be observed for residence and flushing times of canal and bay water with R^2 values of at least 0.859 (Fig. 9). These clear relationships, and the lack of discernible relationships when grouping all three seasons together, reflect the different mechanisms of seaward exchange that occur during the windy season.

4. Discussion

4.1. Model improvement

In consideration of the highly dynamic and stratified thermohaline structure of Cartagena Bay, it may be stated that the model performed quite well. The model's performance could be further improved though, specifically in its prediction of surface salinity and vertical temperature gradients. Inconsistencies in the model's reproduction of surface salinities were expected as there were additional sources of freshwater not considered in the model, including a series of smaller canals flowing from the industrial sector along the bay's east coast, surface runoff from the small catchment area of the bay itself, and occasional discharges from the city's sewerage system through an outdated submarine outfall and backup outlets along the coast when the system overflows. While the influence of the submarine outfall was not detected in the subsurface salinity values of this study's monitoring results, the model's bias to overestimate surface salinity demonstrates the influence of additional freshwater sources which should be incorporated.

The model's ability to reproduce vertical temperature profiles would benefit from further investigation, particularly in consideration of the transitional season simulation. While monitoring results showed that this season had the strongest vertical temperature gradient (Figs. 2 and

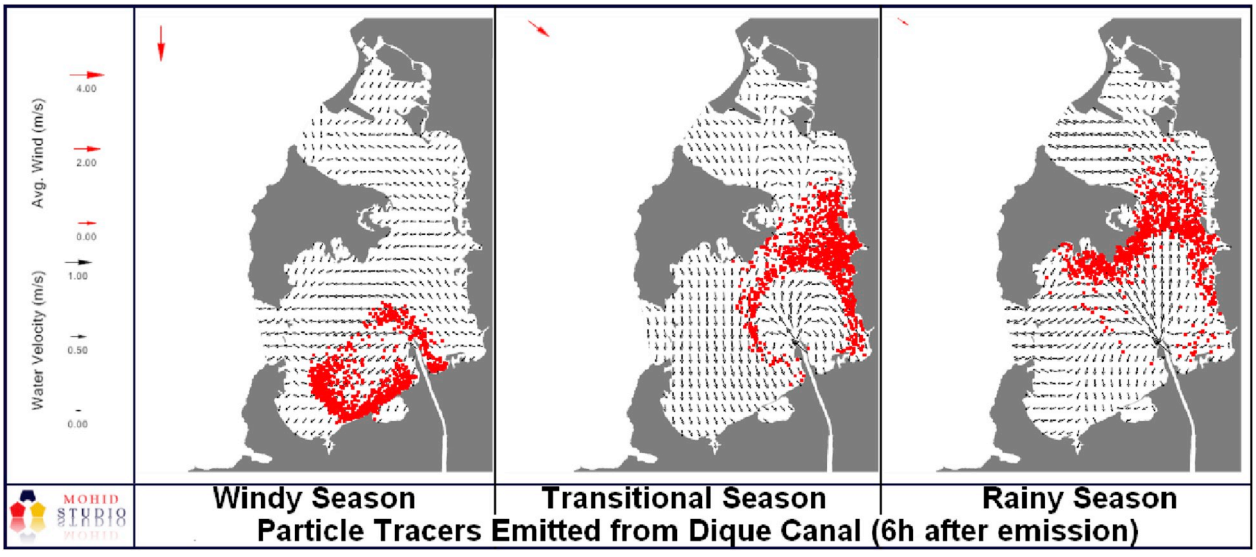

Fig. 7. Evolution of particle tracers six hours after emission from the Dique Canal in the windy (left), transition (center) and rainy (right) season simulations. Wind conditions (mean speed and direction) during the six-hour period and instantaneous surface water velocities are also presented.

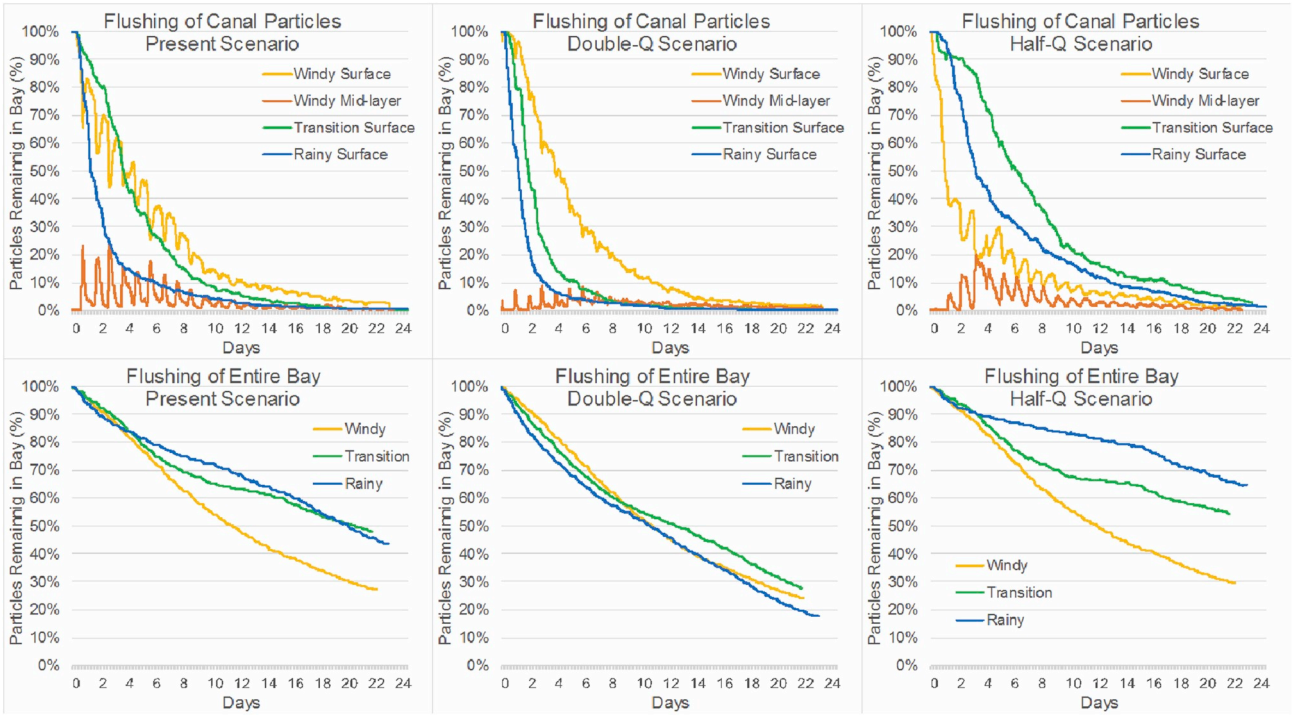

Fig. 8. Evolution of particle tracers emitted from the Dique Canal (above) and throughout the entire bay (below) in the present (left), double-discharge (center) and half-discharge (right) scenarios for three seasons. Windy season particles emitted from the Dique Canal (above: yellow and orange lines) are divided between surface and sub-surface (< 5 m) depths to illustrate vertical exchange through tidal oscillation. (For interpretation of the references to colour in this figure legend, the reader is referred to the Web version of this article.)

3a), modelling results produced a less pronounced thermal stratification (Appendix A). Given the importance of water transparency on the penetration of solar radiation through surface waters, the model could be improved by incorporating the transport of suspended sediments which play a prominent role in the bay's water transparency. The effect of these sediments on water transparency was considered in the present study by calculation of the short-wave light extinction coefficient (K_d) with field measurements of total suspended solids (TSS), however, K_d values were computed using monthly mean TSS surface concentrations and held spatio-temporally constant during the simulation period. By incorporating TSS as a water property transported in the model, K_d values could be calculated independently for each cell and at each time-step, thus incorporating the spatio-temporal variability of water transparency into the model's computations of heat fluxes.

Model calibration could also benefit from additional investigation. While further exploration of parameters found to be less sensitive (surface water roughness, horizontal advection methods) may be inconsequential, continued evaluation of the more sensitive parameters, horizontal viscosity and bottom roughness, may be considered a relevant topic for future research. Coefficients for particle turbulence in the model's Lagrangian transport could also be optimized through calibration with field measurements, as the current study utilized default values known to have worked well in similar coastal systems. Lastly, model calibration based on measured velocity fields in the bay could also be attempted and compared to this study's results.

4.2. Hydrodynamic phenomena

The small differences observed between modelled and measured water levels were prevalent at peaks of high and low water, while the frequency of the tidal signal was quite well matched. These differences may be associated with local and offshore meteorological anomalies, such as storms, waves and atmospheric pressure systems, as well as additional sources of freshwater discharge. Nevertheless, values of MAE (0.031–0.039 m) and RMSE (0.039–0.048 m) were quite low, suggesting that these differences were of minimal consequence. The result showing higher mean water level in the rainy season is in agreement with the previous work of Torres and Tsimplis (2012) which showed a seasonal cycle of water level along the north coast of South America with a peak in October.

The importance of utilizing a 3D model with a high vertical resolution in order to understand the processes of a sharply stratified system such as Cartagena Bay was demonstrated in this study. Some previous studies which utilized 2D models (Palacio et al., 2010) or vertically integrated their results (Molares and Mestres, 2012a) presented a simplified view of the bay's hydrodynamics based on net fluxes, suggesting that water simply flows into the bay through Bocachica, runs south to north, and flows out through Bocagrande. However, results of the present study show more clearly how dual currents are found at both straits (surface outflow, sub-surface inflow) and that the direction of currents along the bay's north-south axis varies both by depth and by seasonal conditions.

The process of vertical exchange is one of the defining characteristics of the bay's seasonal variability. The rainy and transitional seasons exhibited strong thermohaline stratification, predominantly horizontal water velocities and increased stability in density fields near the surface. These conditions restrict vertical advection and vertical turbulent mixing in the bay and result in shorter time scales for surface water renewal. Conversely, the strong winds and lower freshwater discharge of the windy season result in less thermohaline stratification,

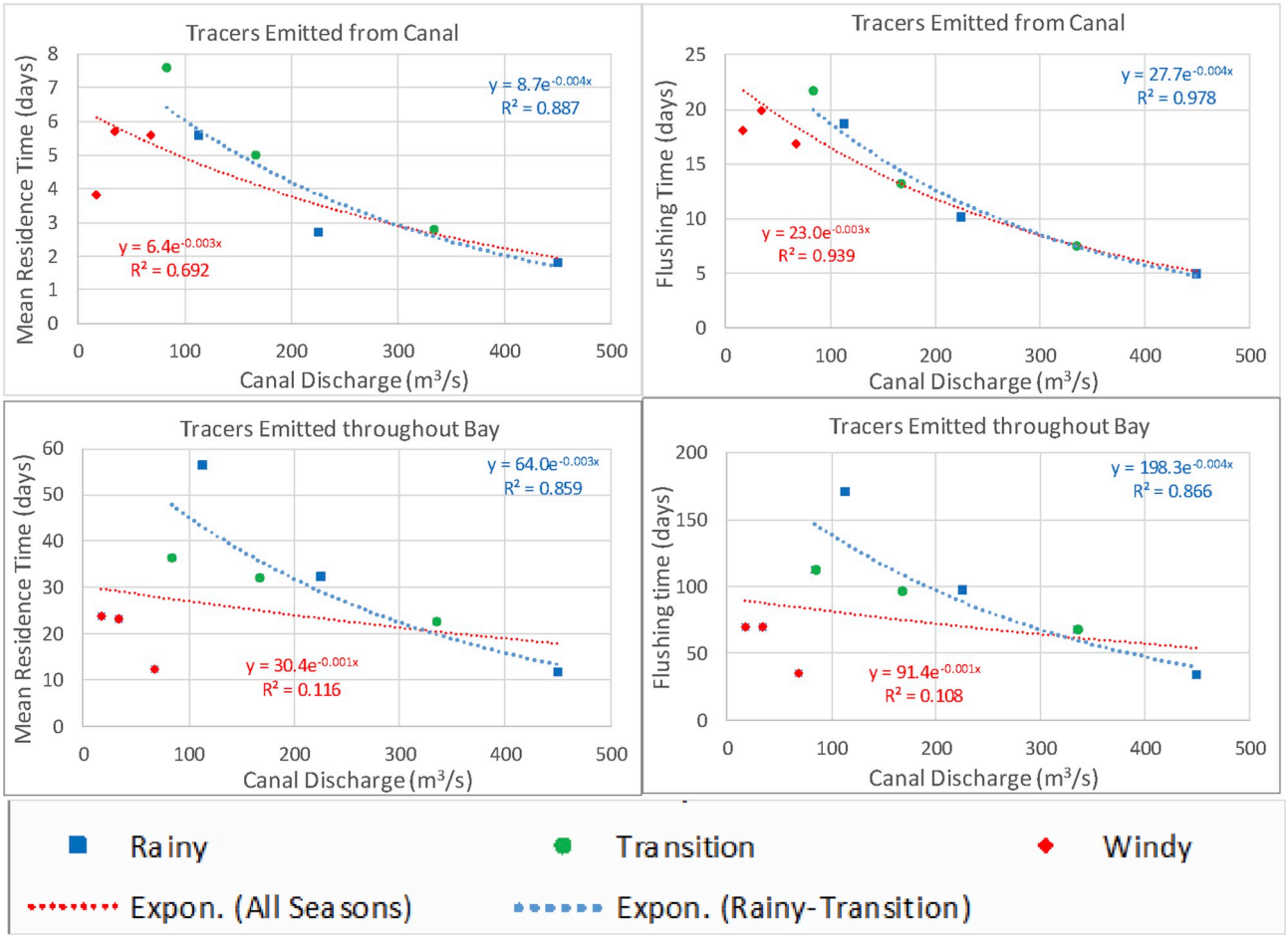

Fig. 9. Relationships between canal discharge and the mean residence times (left) and flushing times (right) of particle tracers emitted from the canal (above) and throughout the entire bay (below). Blue trend lines correspond to a grouping of the Rainy and Transitional season, while red trend lines correspond to a grouping of all three seasons. (For interpretation of the references to colour in this figure legend, the reader is referred to the Web version of this article.)

a shallowing of the pycnocline and greater instability in the water column, which in turn permit the penetration of turbulent diffusion below the surface. This process likely occurs as a positive feedback loop, as the reduction in stratification permits more vertical mixing and increased vertical mixing further reduces stratification. The wind-driven accumulation of water in the southwest part of the bay (Fig. 4) probably also contributes to this process as it causes a gradient in water level which would generate downwelling that transports surface waters to depth. Under these conditions, velocity fields throughout the bay experience increased vertical velocities and highly fluctuating circulation patterns, which result in shorter time scales for water renewal of the bay's overall volume.

The exchange between surface and sub-surface waters was clearly illustrated by the evolution of particle tracers emitted from the canal, which showed substantial vertical exchange during the windy season scenarios though almost none during the other seasons (Fig. 8). This vertical transport coincided with tidal oscillation and was most prevalent under the present and half-discharge scenarios of the windy season. While tidal forces were also present during the rainy and transitional seasons, it appears that the strong vertical stratification during these seasons, along with the increased stratification of the windy double-discharge scenario, caused resistance to vertical mixing. As vertical exchange during the present and half-discharge scenarios of the windy season were quite similar, this suggests that there is a threshold value of freshwater discharge between the present (33.9 m^3/s) and double-discharge scenario (67.7 m^3/s) at which point vertical stratification becomes strong enough to result in resistance to vertical advection.

4.3. Factors controlling water renewal

Modelling results show that freshwater discharge is a principal factor controlling water renewal in Cartagena Bay. This effect is particularly well-defined in the water renewal of surface waters, as tracer particles emitted from the canal were flushed out of the bay faster with increased discharge levels (Fig. 9). However, as observed during the windy season scenarios, under low-discharge conditions the freshwater discharge level is no longer the controlling factor, as has been found in other coastal systems as well (Janeiro et al., 2008). A potential explanation for the reduced effect of discharge on surface water renewal times during windy season scenarios could be that because the strong northerly winds confine the tracer particles within the southern lobe of the bay (Fig. 7), their transport towards the seaward straits becomes more random and less dependent on discharge-driven surface velocities.

Water renewal of the bay's complete volume differs from that of surface waters due to the effect of vertical mixing (Fig. 7). Under the medium- and high-discharge levels of the transitional and rainy season

scenarios, respectively, increased discharge resulted in reduced time scales. However, some of the shortest time scales for water renewal of the complete bay were found with the windy season scenarios, despite their low-discharge levels. Therefore, while surface water flushing is almost completely dependent on discharge levels, the flushing of the bay's total volume is dependent on both discharge levels and wind-driven vertical circulation, the latter of which becomes more important at low-discharge levels.

The effect of the winds as a factor controlling water renewal was also evident in modelling results. For instance, the water renewal times for the windy season double-discharge scenario were shorter than those of the transitional season half-discharge scenario, despite the fact that the former had a lower mean discharge of 67.7 m^3/s than the latter's 83.7 m^3/s (Table 2). This difference, contrary to the general discharge-renewal time relationship (Fig. 9), may be attributed to the influence of the winds on increasing surface water velocities and vertical exchange. Similarly, under the transitional season half-discharge scenario, the mean residence time (36.6 days) and flushing time (113.4 days) of the overall bay are shorter than those of the rainy season half-discharge scenario (56.3 and 171.8 days, respectively), again despite the fact that the former has a lower mean discharge (83.7 m^3/s) than the latter (112.5 m^3/s). While the greater discharge of the rainy season half-discharge scenario did result in shorter water renewal times for the canal water, the transitional season half-discharge scenario generated shorter water renewal times for the overall bay, presumably due to the effect of stronger winds on vertical exchange. Therefore, while canal discharge appears to be the dominant factor controlling water renewal in the bay, under similar discharge conditions the factor of winds becomes prevalent.

Tidal exchange is also known to be a common factor controlling residence times (Rynne et al., 2016). Although the tides are small in Cartagena Bay, instantaneous velocity fields showed increased outflow during ebb tides and the tidal effect on vertical mixing was prominent under low-discharge conditions (Fig. 8). However, as the model simulations were run for complete lunar cycles, tidal effects on residence times would only result in temporal variability within the simulation period, which should balance out in the final result.

4.4. Implications of development scenarios

4.4.1. Increased freshwater discharge

Modelling results show that an increase in upstream watershed runoff, which has been projected for future years (Restrepo et al., 2018), would reduce water renewal time scales in the bay, for both the case of canal waters and the bay's overall volume. This result may be expected in the case of canal water as increased discharge would result in faster surface water velocities that flush the freshwater out of the bay at a higher rate. Reduced time scales for the renewal of the bay's entire water volume, however, may not be as intuitively foreseen because increased freshwater discharge would also cause stronger thermohaline stratification which restricts vertical mixing. Yet model results show that freshwater discharge is a primary factor controlling water renewal in the bay under scenarios of increased runoff. Given that the bay's seaward outflow occurs almost exclusively at surface depths, a potential explanation of this result could be that despite decreases in vertical advection and turbulent mixing due to stronger stratification, when particles finally do rise to the surface layers their seaward flushing by faster surface velocities is achieved in a time scale that outweighs the time lost due to slower vertical circulation.

Though the double-discharge scenario results show that the bay's water renewal would improve as runoff continues its increasing tendency over time, it is essential to recall that the Dique Canal is also one of the bay's principal sources of pollution. Therefore, the implication of this scenario on the bay's water quality is more complex as increased discharge is also likely to bring greater amounts of pollution to the bay. Furthermore, the behavior of pollutants in the bay would differ from the behavior of passive particles due to additional processes such as gravitational percolation, chemical reactions and biological cycling. The question then becomes in regard to the balance that would eventually be reached between increases in both pollution and water renewal rates. Further research using water quality models is recommended to evaluate this question.

4.4.2. Reduced freshwater discharge

Presented with the scenario of the upstream hydraulic intervention planned to reduce freshwater flows into the bay by constructing hydraulic doors along the Dique Canal (Fondo Adaptación, 2018), modelling results show that this would affect the bay by increasing water renewal time scales. This result of longer water renewal time scales due to decreased freshwater discharge may be explained by discharge level being a principal controlling factor on the bay's hydrodynamic processes. This relationship was clear for rainy and transitional season conditions, though discharge level becomes less of a controlling factor under low-discharge conditions thus having minimal effect on the windy season's water renewal times.

These results suggest that the plan to improve Cartagena Bay's pollution issues by constructing hydraulic doors upstream in the canal may be flawed. Such a plan would surely reduce the sediment and pollution loads flowing into the bay from the watershed. However, the increased water renewal time scales that would result from decreased discharge-driven water velocities in the bay could in fact worsen the bay's water quality. This risk has been suggested by other authors (Gómez et al., 2009; Grisales et al., 2014) and previously demonstrated using water quality models (Lonin and Tuchkovenko, 1998; Tuchkovenko et al., 2000, 2002; Tuchkovenko and Lonin, 2003). These modelling studies evaluated various mitigation options and found that the best solution would be to reduce upstream discharge but only in combination with the elimination of local sources of industrial and domestic wastewater, without which the reduction of upstream discharge would result in increased eutrophication and a worsening of oxygen conditions in the bay. The present study corroborates these findings as increased water renewal time scales under reduced discharge scenarios would inhibit the bay's mixing and oxygenation, while the continuous input of local sources of domestic and industrial wastewater (Tosic et al., 2018) could maintain or worsen the bay's multifactorial pollution issues.

4.5. Management recommendations

This study provides a valuable step in the development of coastal management tools for Cartagena Bay. The application of the hydrodynamic model permitted the identification of risks associated with the upstream anthropogenic impacts on freshwater runoff and how these changes can affect the bay's hydrodynamic processes. The assessment of such modifications to coastal circulation is particularly relevant as semi-enclosed coastal water bodies are quite vulnerable to changes in water renewal rates (Dettmann, 2001; Anthony et al., 2009; Newton et al., 2014). For the continued development of modelling tools for the management of Cartagena Bay, it would be recommended to carry out further studies in water quality modelling and operational modelling (e.g. Kenov et al., 2014) which could provide environmental authorities and stakeholders with a real-time early warning system.

The most urgent solution needed for the mitigation of upstream increases in runoff, sediment and pollution loads is improved management of the Magdalena watershed. This is both a daunting and challenging task due to the basin's large scale, widespread population

and diverse anthropogenic activities, and so integrated management of this watershed would require collaboration between a great number of municipal and regional governments and environmental authorities. Currently, there is no such initiative for the joint management of this watershed that is being effectively implemented. Nevertheless, the increasing trends in fluvial fluxes from the watershed (Restrepo et al., 2018) associated with land-cover changes and deforestation (Restrepo et al., 2015) along with the potential for further runoff increases due to climate change and intensification of the El Niño-Southern Oscillation (IPCC et al., 2014; Paeth et al., 2008; Restrepo et al., 2018) make the need for integrated watershed management urgent.

Considering that the plan to reduce freshwater discharges by constructing upstream hydraulic doors could in fact worsen water quality issues in Cartagena Bay, it is crucial to focus efforts on the reduction of local pollution sources. While many of these local wastewater sources have begun to discharge their wastewater to the city's sewage system which flows out to sea north of the city, a large many sources continue to discharge into the bay, as does the city sewage system itself when it overflows. The number of wastewater sources may in fact be increasing as residential populations and the industrial sector are likely growing faster than the city's sewage system. Meanwhile, the wastewater sources that continue to discharge into the bay do so with little to no control on their effluents. As such, there is an urgent and long-standing need for the development of effluent control policies in Cartagena Bay (Tosic et al., 2019, 2018).

Unfortunately, there appears to be a lack of balance in the progress of economic activities and management plans in Cartagena. On the one hand, new industries and ports have rapidly been developed in Cartagena Bay in recent years. On the other hand, the city has yet to successfully complete a development plan over the past seven years, in which time the city has had 10 different mayors, many of whom have faced scandals of alleged corruption. In this light, perhaps the unbalanced development of Cartagena Bay should not be surprising, though by no means should it be condoned.

5. Conclusions

The approach presented in this study was successfully applied to the assessment of water renewal times and future mitigation scenarios, which represent important knowledge needed by environmental managers and decision makers. The pollution issues studied in Cartagena Bay are commonly found in other highly populated coastal areas of the Wider Caribbean Region. This approach could also be applied to other tropical bays in the region facing similar environmental challenges and thus contribute towards resolving common issues in the Caribbean.

Cartagena bay is characterized by strong thermohaline stratification created by fluxes of freshwater runoff and surface heating which inhibit vertical circulation for most of the year. Variability in these fluxes and winds create distinct seasonal conditions. Rainy season conditions consist of high levels of freshwater runoff from the Dique Canal which generate strong vertical density gradients, a deepening of the pycnocline, increased stability in the water column's density structure and heightened water levels in the canal outlet area. These conditions result in increased horizontal velocities which predominantly flow northwards and westwards to the bay's seaward straits where the outflow of less saline surface water is balanced by the inflow of sub-surface seawater. Most of this seawater flows into the bay occur through the southern strait, Bocachica, due to the depth of its navigation canal while the inflow through the northern strait, Bocagrande, is limited by its sub-surface seawall. These conditions are mostly maintained in the transitional season though an increase in northerly winds and decreased freshwater discharge result in an increased westward component in surface flow towards the bay's southern strait.

Further strengthening of northerly winds and reductions in freshwater discharge during the windy season have a much greater effect on the bay's conditions. This season is characterized by much weaker vertical density gradients, a shallowing of the pycnocline and an unstable density structure in the water column. These conditions permit greater vertical exchange generated by wind-driven turbulence and tidal oscillation. Circulation within the bay changes drastically in this season with increased vertical velocities and highly fluctuating circulation patterns. On the surface, the intensification of winds and reduced discharge result in predominantly southwestward currents and heightened water levels in the bay's southwest lobe. This concentrates seaward flow in the southern strait which causes various features (surface outflow, sub-surface inflow and an associated sub-surface anticyclonic eddy) to all occur at lower depths.

Presently, water flowing from the Dique Canal has a mean residence time of 3–6 days and a flushing time of 10–20 days. The variability of these time scales is strongly dependent on canal discharge levels. Meanwhile, the bay's entire water volume has a mean residence time of 23–33 days and a flushing time of 70–99 days. These time scales for the water renewal of the bay's entire volume are principally dependent on discharge level, while wind speed becomes a more prevalent factor at low-discharge levels.

The assessment of future scenarios showed that increases in freshwater runoff caused by human development in the upstream watershed would result in faster water renewal in the bay, while plans to decrease freshwater discharge by constructing hydraulic doors would result in slower water renewal in the bay. Therefore, ongoing plans to mitigate pollution issues in Cartagena Bay by reducing freshwater discharges could in fact worsen the bay's water quality issues as local wastewater discharged into the bay would remain in the system for longer time periods. In this consideration, there is an urgent need for the reduction of local pollution sources and effluent control policies in Cartagena Bay.

While current trends of increasing fluvial fluxes from the upstream watershed would result in faster water renewal times, these fluxes would also be accompanied by greater pollution loads flowing from the canal into the bay. But would these increased water renewal rates be capable of assimilating the increased pollution? One could postulate with regards to the balance that would eventually be reached between these fluvial alterations, and such hypotheses could be evaluated with studies of water quality modelling. In the meantime, there is a long-standing need for improved management of the Magdalena watershed, which is essential to the water resources of Colombia regardless of future scenarios in Cartagena Bay.

Acknowledgements

This work was carried out with the aid of a grant from the International Development Research Centre, Ottawa, Canada (grant number 108747-001). Financial support was also provided by EAFIT University, Corporación Autónoma Regional del Canal del Dique (CARDIQUE; agreement number 15601), as well as a scholarship granted to the lead author by the Erasmus Mundus Doctoral Programme in Marine and Coastal Management (MACOMA). Bathymetry data was collected in the field by the Hydraulic Department of EAFIT University. The authors thank the following persons and organizations for their support in this study: João Janeiro, Francisco Campuzano, Guilherme Franz, Robson Ventura de Souza, Lígia Pinto, Paulo Chambel, John Bairon Ospina, Rogger Escobar, Mariana Jaramillo, Jesús Pérez, Carlos Gutiérrez, Fundación Hernán Echavarría Olózoga, Escuela Naval de Cadetes “Almirante Padilla”, the University of Wyoming's surface observation service and U. Lisboa's Marine Environment Technology Center (MARETEC).

Appendix A. Comparison of Model Results and Measurements

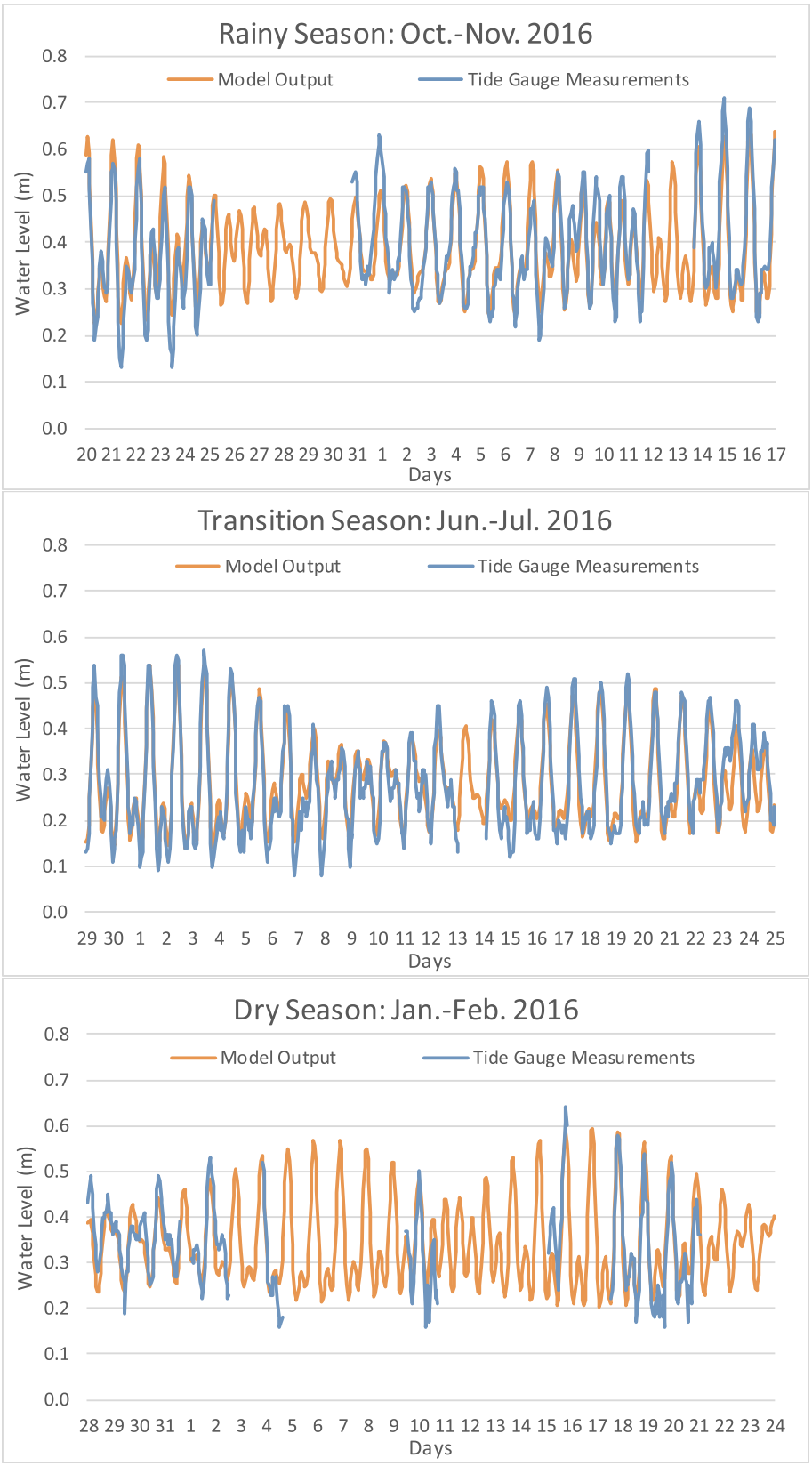

Fig. A.1. Model results compared to measurements of water height during three simulations (rainy, transition, windy seasons) at the tide gauge in Cartagena Bay (Fig. 1).

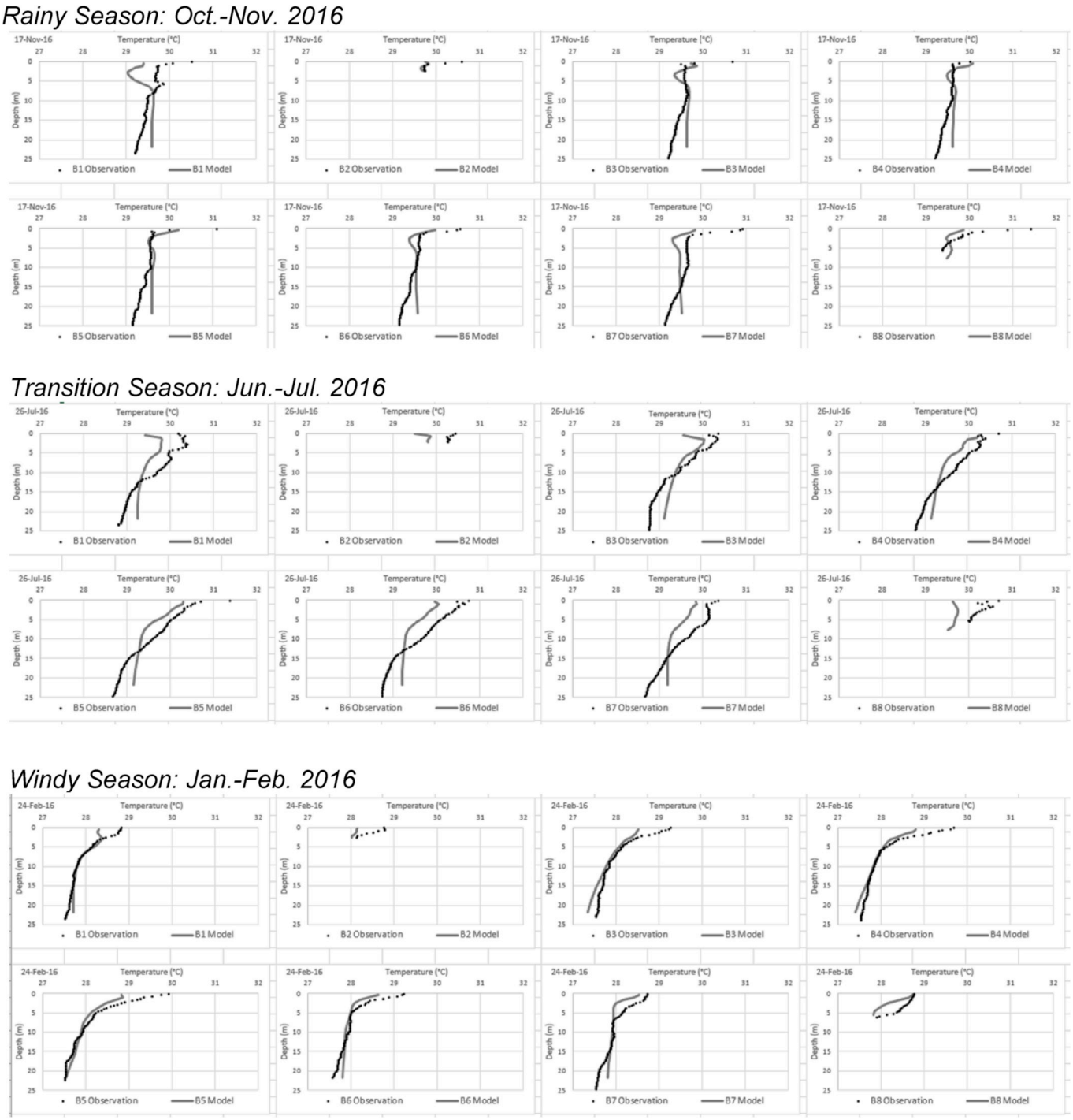

Fig. A.2. Model results compared to measurements of temperature profiles at the end of three simulations (rainy, transition, windy seasons) at eight stations in Cartagena Bay (B1-B8).

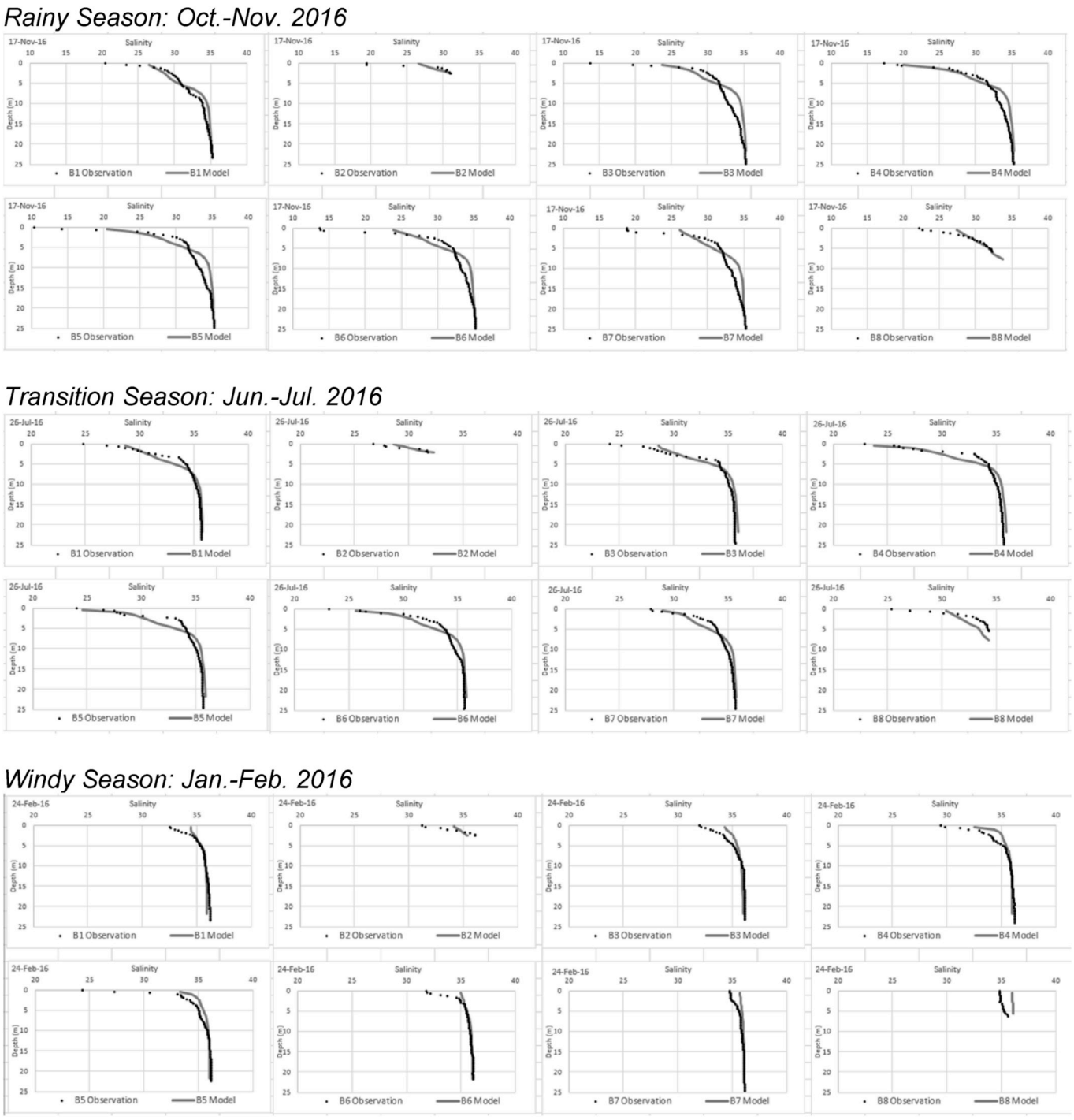

Fig. A.3. Model results compared to measurements of salinity profiles at the end of three simulations (rainy, transition, windy seasons) at eight stations in Cartagena Bay (B1-B8).

References

APHA – American Public Health Association, 1985. Standard Methods for the Examination of Water and Wastewater. American Public Health Association, Washington DC, USA.

Alonso, D., Pineda, P., Olivero, J., Gonzalez, H., Campos, N., 2000. Mercury levels in muscle of two fish species and sediments from the Cartagena Bay and the Ciénaga Grande de Santa Marta, Colombia. Environ. Pollut. 109, 157–163.

Andrade, C.A., Barton, E.D., 2005. The Guajira upwelling system. Cont. Shelf Res. 25, 1003–1022.

Andrade, C.A., Arias, F., Thomas, Y.F., 1988. Nota sobre la turbidez, circulación y erosión en la región de Cartagena (Colombia). Bol. Cient. CIOH 8, 71–82.

Andrade, C.A., Thomas, Y.F., Lerma, A.N., Durand, P., Anselme, B., 2013. Coastal flooding hazard related to swell events in Cartagena de Indias, Colombia. J. Coast. Res. 29 (5), 1126–1136.

Andrade, C.A., Ferrero, A.J., León, H., Mora, H., Carvajal-Perico, H., 2017. Sobre cambios en la línea de costa entre 1735 y 2011 y la subsidencia en la Bahía de Cartagena de Indias, Colombia. Revista de la Academia Colombiana de Ciencias Exactas. Fís. Nat. 41 (158), 94–106.

Anthony, A., Atwood, J., August, P., Byron, C., Cobb, S., Foster, C., Fry, C., Gold, A., Hagos, K., Heffner, L., Kellogg, D., et al., 2009. Coastal lagoons and climate change: ecological and social ramifications in US Atlantic and Gulf coast ecosystems. Ecol. Soc. 14 (1).

Arhonditsis, G.B., Brett, M.T., 2004. Evaluation of the current state of mechanistic aquatic biogeochemical modeling. Mar. Ecol. Prog. Ser. 271, 13–26.

Arhonditsis, G., Tsirtsis, G., Angelidis, M.O., Karydis, M., 2000. Quantification of the effects of nonpoint nutrient sources to coastal marine eutrophication: applications to a semi-enclosed gulf in the Mediterranean Sea. Ecol. Model. 129 (2–3), 209–227.
Braunschweig, F., Martins, F., Chambel, P., Neves, R., 2003. A methodology to estimate renewal time scales in estuaries: the Tagus Estuary case. Ocean Dynam. 53 (3), 137–145.
Burchard, H., 2002. Applied Turbulence Modelling in Marine Waters, vol. 100 Springer Science & Business Media.
Cañon Páez, M.L., Tous, G., Lopez, K., Lopez, R., Orozco, F., 2007. Variación espacio-temporal de los componentes fisicoquímico, zooplanctónico y microbiológico en la Bahía de Cartagena. Bol. Cient. CIOH 25, 120–134.
Cardique, AGD, 2006. Registro de las actividades de desarrollo de la franja costera de la parte continental de la Bahia de Cartagena - Departamento de Bolívar. Corporación Autonoma Regional del Canal del Dique (Cardique) & Fundación Alta Gestión Para el Desarrollo (AGD). Informe Final. Cartagena de Indias, pp. 204.
Castro, L.A., 1997. Estudio de la contaminación por pesticidas, en ecosistemas costeros en el area de Cartagena, Cienaga de la Virgen y zona agrícola adyacente. Bol. Cient. CIOH 18, 15–22.
Cogua, P., Campos-Campos, N.H., Duque, G., 2012. Concentración de mercurio total y metilmercurio en sedimento y seston de la Bahía de Cartagena, Caribe Colombiano. Bol. Invest. Mar. Cost. 41 (2), 267–285 ISSN 0122-9761.
Cucco, A., Umgiesser, G., 2006. Modeling the Venice Lagoon residence time. Ecol. Model. 193 (1–2), 34–51.
Delhez, É.J., Heemink, A.W., Deleersnijder, É., 2004. Residence time in a semi-enclosed domain from the solution of an adjoint problem. Estuar. Coast. Shelf Sci. 61 (4), 691–702.
Dettmann, 2001. Effect of water residence time on annual export and denitrification of nitrogen in Estuaries: a model analysis Estuaries. 24 (4), 481–490.
Devlin, M.J., Barry, J., Mills, D.K., Gowen, R.J., Foden, J., Sivyer, D., Tett, P., 2008. Relationships between suspended particulate material, light attenuation and Secchi depth in UK marine waters. Estuar. Coast. Shelf Sci. 79 (3), 429–439.
Díaz, J.M., Gómez, D.I., 2003. Cambios históricos en la distribución y abundancia de praderas de pastos marinos en la bahía de Cartagena y áreas aledañas (Colombia), vol. 32. Boletín del Instituto de Investigaciones Marinas y Costeras – INVEMAR, pp. 57–74.
FAO & CCO, 1978. Study concerning the mercury pollution of the Cartagena bay. Pollution assessment project. Organización de las Naciones Unidas para la Alimentación y la Agricultura (FAO) y Comisión Colombiana Oceanográfica (CCO). Swedish Water and Air Pollution Research Institute, Estocolmo, pp. 63.
Ferrarin, C., Bergamasco, A., Umgiesser, G., Cucco, A., 2013. Hydrodynamics and spatial zonation of the Capo Peloro coastal system (Sicily) through 3-D numerical modeling. J. Mar. Syst. 117, 96–107.
Fondo Adaptación, 2018. Online Resource. accessed 6/june/2018. http://sitio.fondoadaptacion.gov.co/index.php/el-fondo/macroproyectos/canal-del-dique.
Franz, G.A.S., Leitão, P., Santos, A.D., Juliano, M., Neves, R., 2016. From regional to local scale modelling on the south-eastern Brazilian shelf: case study of Paranaguá estuarine system. Braz. J. Oceanogr. 64 (3), 277–294.
Garay, J., 1983. Concentracion y Composicion de Hidrocarburos Derivados del Petroleo en Aguas Sedimentos y Peces de la Bahia de Cartagena. Bol. Cient. CIOH 6, 41–62.
Garay, J., Giraldo, L., 1997. Influencia de los aportes de material orgánico externa y autoctona en el decrecimiento de los niveles de oxígeno disuelto en la bahía de Cartagena, Colombia. Bol. CIOH 18, 1–13 ISSN 0120 0542.
Gómez, A., Osorio, A.F., Toro, F.M., Osorio, J.D., Álvarez, O.A., 2009. Efecto del cambio de los caudales del Canal del Dique sobre el patrón de transporte horizontal en la bahía de Barbacoas. Bol. Cient. CIOH 27, 90–111.
Grisales, C.H., Salgado, J.A., Molares, R.J., 2014. Proceso de intercambio de masas de agua de la bahía de Cartagena (Caribe colombiano) basado en la medición de parámetros oceanográficos. Bol. Cient. CIOH 32, 47–70.
Guerrero, E., Restrepo, M., Podlesky, E., 1995. Contaminación por mercurio de la Bahía de Cartagena. Biomedica 15, 144–154.
IPCC, 2014. In: Pachauri, R.K., Meyer, L.A. (Eds.), Climate Change 2014: Synthesis Report. Contribution of Working Groups I, II and III to the Fifth Assessment Report of the Intergovernmental Panel on Climate Change [Core Writing Team. IPCC, Geneva, Switzerland, pp. 151.
Jackson, J.B.C., Donovan, M.K., Cramer, K.L., Lam, V.V. (Eds.), 2014. Status and Trends of Caribbean Coral Reefs: 1970-2012. Global Coral Reef Monitoring Network. IUCN, Gland, Switzerland, pp. 304.
James, I.D., 2002. Modelling pollution dispersion, the ecosystem and water quality in coastal waters: a review. Environ. Model. Softw 17 (4), 363–385.
Janeiro, J., Fernandes, E., Martins, F., Fernandes, R., 2008. Wind and freshwater influence over hydrocarbon dispersal on Patos Lagoon, Brazil. Mar. Pollut. Bull. 56 (4), 650–665.
Jaramillo-Colorado, B.E., Arroyo-Salgado, B., Ruiz-Garces, L.C., 2015. Organochlorine pesticides and parasites in Mugil incilis collected in Cartagena Bay, Colombia. Environ. Sci. Pollut. Control Ser. 22 (22), 17475–17485.
Jaramillo-Colorado, B.E., Aga, D.S., Noguera-Oviedo, K., 2016. Heavy metal contamination of estuarine sediments from Cartagena Bay, Colombia. Toxicol. Lett. 259, S170. ISSN 0378-4274. https://doi.org/10.1016/j.toxlet.2016.07.405.
Johnson-Restrepo, B., Olivero-Verbel, J., Lu, S., Guette-Fernandez, J., Baldiris-Avila, R., O'Byrne-Hoyos, I., Aldous, K.M., Addink, R., Kannan, K., 2008. Polycyclic aromatic hydrocarbons and their hydroxylated metabolites in fish bile and sediments from coastal waters of Colombia. Environ. Pollut. 151, 452–459.
Jouon, A., Douillet, P., Ouillon, S., Fraunié, P., 2006. Calculations of hydrodynamic time parameters in a semi-opened coastal zone using a 3D hydrodynamic model. Cont. Shelf Res. 26 (12–13), 1395–1415.
Karydis, M., Kitsiou, D., 2013. Marine water quality monitoring: a review. Mar. Pollut. Bull. 77 (1–2), 23–26.
Kenov, I.A., Campuzano, F., Franz, G., Fernandes, R., Viegas, C., Sobrinho, J., de Pablo, H., Amaral, A., Pinto, L., Mateus, M., Neves, R., 2014. Advances in modeling of water quality in estuaries. In: Remote Sensing and Modeling. Springer, Cham, pp. 237–276.
Lee, H.W., Park, S.S., 2013. A hydrodynamic modeling study to estimate the flushing rate in a large coastal embayment. J. Environ. Manag. 115, 278–286.
Leitão, P.C., Mateus, M., Braunschweig, F., Fernandes, L., Neves, R., 2008. Modelling coastal systems: the MOHID Water numerical lab. In: Neves Baretta, R.J., Mateus, M. (Eds.), Perspectives on Integrated Coastal Zone Management in South America. IST Press, Lisbon, pp. 77–88 2008.
Lonin, S., 1997a. Cálculo de la transparencia del agua en la bahía de Cartagena. Bol. Cient. CIOH 18, 85–92.
Lonin, S.A., 1997b. Hydrodynamic modelling and the problem of oil spills on the Colombian Caribbean shoreline. Spill Technol. Newslett. 22, 1–6.
Lonin, S.A., 1999. Lagrangian model for oil spill diffusion at sea. Spill Sci. Technol. Bull. 5 (5–6), 331–336.
Lonin, S.A., 2009. Modelación numérica en oceanología. Dirección General Marítima – Centro de Investigaciones Oceanográficas e Hidrográficas. In: DIMAR, Serie Publicaciones Especiales CIOH, vol. 7. Cartagena de Indias, D. T. y C, pp. 169.
Lonin, S., Parra, C., 2005. Predicción del comportamiento de las manchas de hidrocarburo derramado en el mar. Bol. CIOH 23, 6–21.
Lonin, S., Tuchkovenko, Y., 1998. Modelación matemática del régimen de oxígeno en la bahía de Cartagena. Avances en Rec. Hid. 5, 1–16.
Lonin, S., Parra, C., Andrade, C., Thomas, I., 2004. Patrones de la pluma turbia del canal del Dique en la bahía Cartagena. Bol. CIOH 22, 77–89.
Lyard, F., Lefèvre, F., Letellier, T., Francis, O., 2006. Modelling the global ocean tides: modern insights from FES2004. Ocean Dynam. 56 (5), 394–415.
Martins, F., Leitão, P.C., Silva, A., Neves, R., 2001. 3D modelling in the Sado estuary using a new generic vertical discretization approach. Oceanol. Acta 24, 551–562.
Mateus, M., Neves, R. (Eds.), 2013. Ocean Modelling for Coastal Management: Case Studies with MOHID. IST Press, pp. 165.
Mogollón, J.V., 2013. El Canal del Dique: Historia de un Desastre Ambiental. El Áncora Editores, Bogotá, pp. 197.
Molares, R., 2004. Clasificación e identificación de las componentes de marea del Caribe colombiano. Bol. Cient. CIOH (22), 105–114.
Molares, R., Mestres, M., 2012a. Efectos de la descarga estacional del Canal del Dique en el mecanismo de intercambio de aguas de una bahía semicerrada y micromareal: Bahía de Cartagena, Colombia. Bol. Cient. CIOH 30, 53–74.
Molares, R., Mestres, M., 2012b. La influencia de la descarga del Canal del Dique en los niveles del mar de la Bahía de Cartagena-Colombia. Bol. Cient. CIOH 30, 13–28.
Monsen, N.E., Cloern, J.E., Lucas, L.V., 2003. A comment on the use of flushing time, residence time and age as transport time scales. Limnol. Oceanogr. 47 (5), 1545–1553.
Newton, A., Icely, J., Cristina, S., Brito, A., Cardoso, A.C., Colijn, F., Dalla Riva, S., Gertz, F., Hansen, J.W., Holmer, M., Ivanova, K., 2014. An overview of ecological status, vulnerability and future perspectives of European large shallow, semi-enclosed coastal systems, lagoons and transitional waters. Estuar. Coast. Shelf Sci. 140, 95–122.
Newton, A., Brito, A.C., Icely, J.D., Derolez, V., Clara, I., Angus, S., Schernewski, G., Inácio, M., Lillebø, A.I., Sousa, A.I., Béjaoui, B., et al., 2018. Assessing, Quantifying and Valuing the Ecosystem Services of Coastal Lagoons.
Olivero-Verbel, J., Johnson-Restrepo, B., Baldiris-Avila, R., Guette-Fernandez, J., Magallanes-Carreazo, E., Vanegas-Ramirez, L., Kunihiko, N., 2008. Human and crab exposure to mercury in the Caribbean coastal shoreline of Colombia: impact from an abandoned chlor-alkali plant. Environ. Int. 34, 476–482.
Olivero-Verbel, J., Caballero-Gallardo, K., Torres-Fuentes, N., 2009. Assessment of mercury in muscle of fish from Cartagena Bay, a tropical estuary at the north of Colombia. Int. J. Environ. Health Res. 19 (5), 343–355.
Olivero-Verbel, J., Agudelo-Frias, D., Caballero-Gallardo, K., 2013. Morphometric parameters and total mercury in eggs of snowy egret (Egretta thula) from Cartagena Bay and Totumo Marsh, north of Colombia. Mar. Pollut. Bull. 69, 105–109.
O'Neill, D.W., Fanning, A.L., Lamb, W.F., Steinberger, J.K., 2018. A good life for all within planetary boundaries. Nat. Sustain. 1 (2), 88.
Paeth, H., Scholten, A., Friederichs, P., Hense, A., 2008. Uncertainties in climate change prediction: el Niño-Southern-Oscillation and monsoons. Glob. Planet. Chang. 60, 265–288.
Pagliardini, J.L., Gómez, M.A., Gutiérrez, H., Zapata, S.I., Jurado, A., Garay, J.A., Vernette, G., 1982. Síntesis del proyecto Bahía de Cartagena. Bol. Cient. CIOH 4, 49–110.
Palacio, C., García, F., Garcia, U., 2010. Calibración de un modelo hidrodinámico 2d para la bahía de Cartagena. Dyna 164, 152–166.
Parga-Lozano, C.H., Marrugo-Gonzalez, A.J., Fernandez-Maestre, R., 2002. Hydrocarbon contamination in Cartagena bay, Colombia. Mar. Pollut. Bull. 44, 71–81.
Parsons, T., Takahashi, M., Hargrave, G., 1984. Biological Oceanographic Processes. Pergamon Press, New York, pp. 330p.
Pingree, R.D., Morrison, G.K., 1973. The relationship between stability and source waters for a section in the Northeast Atlantic. J. Phys. Oceanogr. 3 (3), 280–285.
Portela, L.I., 1996. Mathematical Modelling of Hydrodynamic Processes and Water Quality in Tagus Estuary. PhD Thesis. Universidade Técnica de Lisboa, Instituto Superior Técnico, Lisboa, Portugal.
Restrepo, J.D., 2008. Applicability of LOICZ catchment-coast Continuum in a major Caribbean basin: the Magdalena River, Colombia. Estuar. Coast. Shelf Sci. 77, 214-229.
Restrepo, J.D., Kjerfve, B., 2000. Magdalena river: interannual variability (1975–1995) and revised water discharge and sediment load estimates. J. Hydrol. 235 (1), 137–149.

Restrepo, J.D., Zapata, P., Díaz, J.M., Garzón-Ferreira, J., García, C.B., 2006. Fluvial fluxes into the Caribbean Sea and their impact on coastal ecosystems: the Magdalena River, Colombia. Glob. Planet. Chang. 50 (1–2), 33–49.

Restrepo, J.D., Kettner, A., Syvitski, J., 2015. Recent deforestation causes rapid increase in river sediment load in the Colombian Andes. Anthropocene 10, 13–28.

Restrepo, J.C., Escobar, J., Otero, L., Franco, D., Pierini, J., Correa, I., 2016. Factors influencing the distribution and characteristics of surface sediment in the Bay of Cartagena, Colombia. J. Coast. Res. 33 (1), 135–148.

Restrepo, J.D., Escobar, R., Tosic, M., 2018. Fluvial fluxes from the Magdalena River into Cartagena Bay, Caribbean Colombia: trends, future scenarios and connections with upstream human impacts. Geomorphology 302 (92), 105. ISSN 0169-555X. https://doi.org/10.1016/j.geomorph.2016.11.007.

Rueda, J.G., Otero, L.J., Pierini, J.O., 2013. Caracterización hidrodinámica en un estuario tropical de Suramérica con régimen micro-mareal mixto (Bahía de Cartagena, Colombia). Bol. Cient. CIOH 31, 159–174.

Rueda-Roa, D.T., Muller-Karger, F.E., 2013. The southern Caribbean upwelling system: sea surface temperature, wind forcing and chlorophyll concentration patterns. Deep-Sea Res. I 78, 102–114.

Rynne, P., Reniers, A., van de Kreeke, J., MacMahan, J., 2016. The effect of tidal exchange on residence time in a coastal embayment. Estuar. Coast. Shelf Sci. 172, 108–120.

Steen, R.J.C.A., Evers, E.H.G., Van Hattum, B., Cofino, W.P., Brinkman, U.T., 2002. Net fluxes of pesticides from the Scheldt estuary into the north sea: a model approach. Environ. Pollut. 116 (1), 75–84.

Takeoka, H., 1984. Fundamental concepts of exchange and transport time scales in a coastal sea. Cont. Shelf Res. 3, 311–326.

Torres, R.R., Tsimplis, M.N., 2012. Seasonal sea level cycle in the Caribbean Sea. J. Geophys. Res. 117, C07011. https://doi.org/10.1029/2012JC008159.

Tosic, M., Restrepo, J.D., Lonin, S., Izquierdo, A., Martins, F., 2019. Water and Sediment Quality in Cartagena Bay, Colombia: Seasonal Variability and Potential Impacts of Pollution. Estuar., Coast. Shelf Sci. 216, 187–203. ISSN 0272-7714. https://doi.org/10.1016/j.ecss.2017.08.013.

Tosic, M., Restrepo, J.D., Izquierdo, A., Lonin, S., Martins, F., Escobar, R., 2018. An Integrated Approach for the Assessment of Land-Based Pollution Loads in the Coastal Zone Demonstrated in Cartagena Bay, Colombia. Estuar. Coast. Shelf Sci. 211, 217–226. https://doi.org/10.1016/j.ecss.2017.08.035.

Tuchkovenko, Y., Lonin, S.A., 2003. Mathematical model of the oxygen regime of Cartagena Bay. Ecol. Model. 165 (1), 91–106 ISSN 0304-3800.

Tuchkovenko, Y., Lonin, S., Calero, L.A., 2000. Modelación ecológica de las bahías de Cartagena y Barbacoas bajo la influencia del Canal del Dique. Av. Recur. Hidráulicos 7, 76–94.

Tuchkovenko, Y., Lonin, S., Calero, L., 2002. Modelo de eutroficación de la bahía de Cartagena y su aplicación práctica. Bol. Cient. CIOH 20, 28–44.

UNEP-UCR/CEP, 2010. Updated CEP Technical Report No. 33 Land-Based Sources and Activities in the Wider Caribbean Region. pp. 80 CEP Technical Report No. 52.

UNEP/GPA, 2006. The State of the Marine Environment: Trends and Processes. UNEP/GPA, The Hague, pp. 43.

Urbano, J., Thomas, F., Para, C., Genet, P., 1992. Dinámica de la pluma de turbidez del Canal del Dique en la Bahía de Cartagena. Bol. Cient. CIOH 11, 3–14.

Willmott, C.J., 1982. Some comments on the evaluation of model performance. Bull. Am. Meteorol. Soc. 63 (11), 1309–1313.

Willmott, C.J., Matsuura, K., 2005. Advantages of the mean absolute error (MAE) over the root mean square error (RMSE) in assessing average model performance. Clim. Res. 30 (1), 79–82.

Zhang, W., Arhonditsis, G.B., 2008. Predicting the frequency of water quality standard violations using Bayesian calibration of eutrophication models. J. Great Lake. Res. 34 (4), 698–720.

Zimmerman, J.T.F., 1976. Mixing and flushing of tidal embayments in the western Dutch Wadden Sea part I: distribution of salinity and calculation of mixing time scales. Neth. J. Sea Res. 10 (2), 149–191.